Since January 2020 Elsevier has created a COVID-19 resource centre with free information in English and Mandarin on the novel coronavirus COVID-19. The COVID-19 resource centre is hosted on Elsevier Connect, the company's public news and information website.

Biomaterials 146 (2017) 97–114

Contents lists available at ScienceDirect

Biomaterials

journal homepage: www.elsevier.com/locate/biomaterials

Review

State of diagnosing infectious pathogens using colloidal nanomaterials

Jisung Kim [a, b, c], Mohamed A. Abdou Mohamed [a, b, g], Kyryl Zagorovsky [a, b], Warren C.W. Chan [a, b, d, e, f, *]

[a] Institute of Biomaterials and Biomedical Engineering, University of Toronto, Toronto, Ontario M5S 3G9, Canada
[b] Terrence Donnelly Centre for Cellular and Bimolecular Research, University of Toronto, Toronto, Ontario M5S 3E1, Canada
[c] Centre for Global Engineering, University of Toronto, Toronto, Ontario M5S 1A4, Canada
[d] Department of Chemistry, University of Toronto, Toronto, Ontario M5S 3H6, Canada
[e] Department of Chemical Engineering, University of Toronto, Toronto, Ontario M5S 3E5, Canada
[f] Department of Materials Science and Engineering, University of Toronto, Toronto, Ontario M5S 3E4, Canada
[g] Botany and Microbiology Department, Faculty of Science, Zagazig University, Egypt

ARTICLE INFO

Article history:
Received 4 June 2017
Received in revised form
7 August 2017
Accepted 13 August 2017
Available online 17 August 2017

Keywords:
Nanotechnology
Diagnostics
Point of care
Clinical translation
Nanomaterials

ABSTRACT

Infectious diseases are a major global threat that accounts for one of the leading causes of global mortality and morbidity. Prompt diagnosis is a crucial first step in the management of infectious threats, which aims to quarantine infected patients to avoid contacts with healthy individuals and deliver effective treatments prior to further spread of diseases. This review article discusses current advances of diagnostic systems using colloidal nanomaterials (*e.g.*, gold nanoparticles, quantum dots, magnetic nanoparticles) for identifying and differentiating infectious pathogens. The challenges involved in the clinical translation of these emerging nanotechnology based diagnostic devices will also be discussed.

1. Introduction

An infectious disease (ID), also known as a communicable or transmissible disease, is defined as an illness caused by infectious pathogens such as bacteria, virus, fungus, parasite, and prion [1]. There are more than 1400 organisms that cause infection in humans [2–5], and IDs remain as one of the major causes of morbidity and mortality and pose a significant threat to global health and safety [6,7]. In 2009, communicable diseases accounted for 51% of years of life lost (YLL), a measure of premature mortality (Fig. 1) [8]. Interestingly, this number is represented asymmetrically among countries of different income groups. IDs have been reported to be more problematic in low-income countries, where communicable diseases accounted for 68% of YLL compared to only 8% in high-income countries (Fig. 1). However, IDs also cannot be overlooked in the developed world due to the rapid evolution of antimicrobial resistance that render antibiotics less effective against these infections [9,10].

Besides the mortality and YLL, IDs can lead to other consequences such as economic burden due to the loss of worker productivity, and money spent on treatment and replacement of work absences [11,12]. The emergence and re-emergence of IDs will continue to overwhelm the global economy and public health. It has been expected that IDs will remain the most common cause of mortality in the next 25 years, especially in low-income countries [13].

Diagnostics play a crucial role in the management of IDs by providing appropriate information about a patient's disease state, which allows healthcare workers to quarantine infected individuals to prevent further spread of pathogens, and administer appropriate treatments until patients become successfully treated. Nonetheless, the lack of appropriate diagnostics cause poor control over infections in low-income countries, in which undiagnosed or misdiagnosed diseases can spread to other regions of the world with international travels and worsen global morbidity and mortality. Such threats of infectious diseases on a global scale was experienced with Severe Acute Respiratory Syndrome (SARS) pandemic in 2003 [14], H1N1 flu pandemic in 2009 [15], Ebola epidemic in 2014

* Corresponding author. Institute of Biomaterials and Biomedical Engineering, University of Toronto, Toronto, Ontario M5S 3G9, Canada.
E-mail address: warren.chan@utoronto.ca (W.C.W. Chan).

http://dx.doi.org/10.1016/j.biomaterials.2017.08.013
0142-9612/

[16], and Zika outbreak in 2015 [17].

The advancements in nanotechnology developments are offering innovative solutions to improve current diagnostic strategies in the management of IDs. The National Nanotechnology Initiative of the United States defined nanotechnology as the "understanding and control of matter at dimensions between approximately 1 and 100 nm" [18]. At this scale, nanomaterials have tunable optical, magnetic, electrical, thermal and biological properties, and can be engineered with different shapes, sizes, chemical compositions and surface functionalities [19]. These properties enable them to be exploited for improving the detection of biological molecules or whole pathogens. Additionally, nanomaterials have much greater surface-area-to-volume ratios than macroscopic materials [20], which provides a great capacity to functionalize the surface with many molecules. For example, a cube with 1-cm dimensions can be divided into 10^{21} 1-nm cubes, which will increase the surface area by 10 million times [19]. This enables the surface of nanomaterials to be coated with molecules that can selectively bind to the target molecules or pathogens. The applications of nanotechnology for diagnostics is referred to as "nanodiagnostics".

This review highlights conventional methods for diagnosing IDs and explores their limitations. This article will then examine how nanomaterials are being exploited to overcome some of these limitations. The properties of nanomaterials that are commonly exploited in the development of *in vitro* diagnostics, various nanodiagnostic readout signal modalities, and future direction of nanodiagnostics will be discussed.

2. Conventional diagnostic approaches

Effective diagnosis of IDs is important for the successful control and management of diseases [21–23]. Symptomatic infections may be managed without the need for extensive diagnosis; however, this could also lead to overtreatment due to the administration of inappropriate or unnecessary treatment, and risk of developing antimicrobial resistance. Additionally, a disease can be caused by different pathogens that present similar symptoms. For instance, respiratory tract infection can be caused by influenza virus which produces respiratory syndromes that are clinically similar to those caused by streptococci, mycoplasma, or other viruses [24]. As a result, an accurate and rapid identification of infectious pathogens is desirable before the initiation of a treatment [22,24].

Several diagnostic techniques are currently available to determine the causative agents of infectious diseases, guide healthcare professionals to initiate proper treatments, provide control measures to quarantine the infected individuals, and monitor the disease progression. These techniques include microscopy, culture, enzyme-linked immunosorbent assay (ELISA), lateral flow assay (LFA), and polymerase chain reaction (PCR).

2.1. Microscopy

Numerous microscopic techniques are widely used for the diagnosis of infectious diseases like malaria [25–27], tuberculosis [28,29], and urinary tract infections [30–32]. This involves direct examination of either stained or unstained smears (blood, sputum, urine, *etc.*) at the cellular level using a variety of microscopic techniques (*e.g.* bright field, dark field, and fluorescence microscopy). Such techniques have been reported to achieve high level of diagnostic sensitivity for certain pathogens [26,28]; however, their outcomes can strongly vary depending on the training level of a microscopist, concentration of the pathogen within the clinical specimen, staining methods, and other sample preparation steps [27,31]. Hence, manual microscopy may not be a reliable screening method especially when it is performed by non-experts due to its inherent variability [33]. Microscopes can also be expensive with specialized optical features, which make them mostly unavailable in resource-limited and decentralized regions.

2.2. Culture

Culturing has been extensively used for identification of microorganisms in a laboratory. Some microorganisms can be cultured in artificial media (*e.g.* bacteria, yeast and fungi) while others (*e.g.* viruses) require living host such as mammalian cells or living animals for culturing and isolation. Selective culture media that contains specific inhibitors can be used to allow growth of specific bacterial pathogens while inhibiting growth of other flora. Culturing can provide quantitative results by spreading a specific volume of specimen over the surface of agar media and calculating the number of colony forming units per milliliter (CFU/ml). This is a commonly-used method for the identification of bacterial

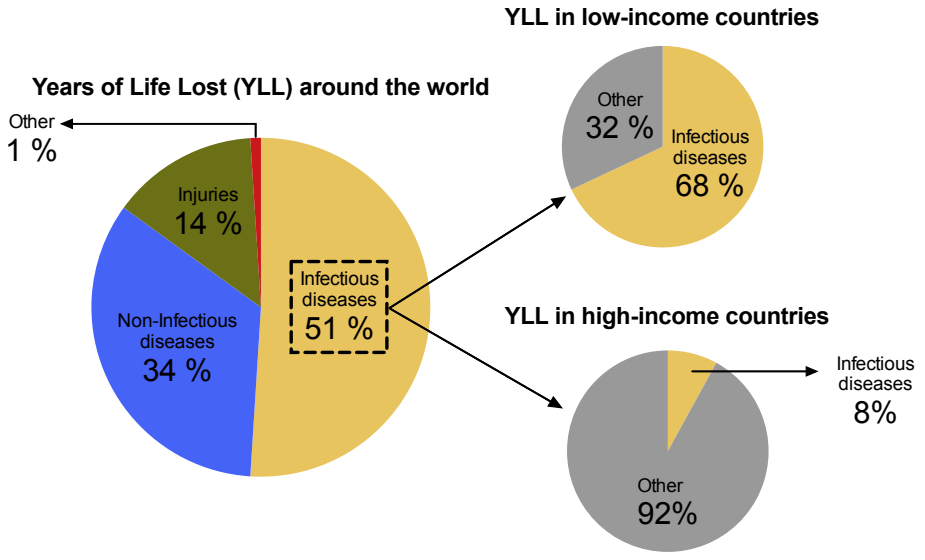

Fig. 1. YLL caused by infectious diseases around the world, in low-income countries and in high-income countries [8].

pathogens associated with a variety of infections.

Culture-based assays are also used to detect antibiotic susceptibility of bacterial infections [34,35]. These phenotypic assays include broth dilution and agar diffusion (*e.g.* antimicrobial gradient diffusion and disc diffusion) methods [36–38]. Broth dilution can be carried out in either macro- (test tubes) or micro-scale (96-well plate), which involves determining the minimum inhibitory concentration (MIC) of an antibiotic in a liquid growth medium inoculated with a bacterial suspension by observing the difference in the solution turbidity after incubation. In the agar diffusion method, a bacterial inoculum is applied on an agar plate, and either a paper antibiotic disc, or a plastic test strip that is embedded with an antibiotic concentration gradient placed on the agar surface. The diameter of inhibition zone qualitatively indicates the susceptibility (*i.e.* either susceptible, intermediate, or resistant) in the disc diffusion method, whereas the MIC is quantitatively measured from the strip in the antimicrobial gradient method for determination of resistance.

The main drawback of culturing is that it is time-consuming (24–72 hours) [34]. Furthermore, some types of bacteria cannot be cultured in a standard laboratory, and therefore cannot be detected using this method [24,39]. Many instruments have been developed to automate the culturing process. Currently there are four commercially available automated instruments approved by the Food and Drug Administration (FDA) for use in the United States: MicroScanWalkAway (Siemens Healthcare Diagnostics), BD Phoenix Automated Microbiology System (BD Diagnostics), Vitek 2 System (bioMe'rieux), and Sensititre ARIS 2X (Trek Diagnostic Systems). Despite having less labor inputs, these instruments are expensive and are only suitable for use in centralized laboratories [36].

2.3. Enzyme-linked immunoassay (ELISA)

Many serological diagnostic tests are performed using ELISA to detect presence of proteins, peptides or antibodies in a biological sample. There are indirect, direct, sandwich, and competitive ELISA. All of these immunoassays involve the use of an enzyme-labeled antibody and a chromogenic substrate of the enzyme that changes the colorimetric or fluorescence signal in the presence of biological molecules (proteins, peptides, *etc.*) [40]. In a typical sandwich ELISA test, the target analyte is sandwiched between a capture antibody immobilized on a solid surface, and an enzyme-linked detection antibody, which converts the substrate to produce a visible color change or a fluorescence signal [41]. The analytical sensitivity of ELISA is in the femto to nano-molar range, which may not be sufficient for diagnosis of certain diseases [42,43]. Also, there are difficulties for practical use of this technique in resource-limited settings since ELISA requires a bulky instrument for the optical detection, expensive antibody reagents, many steps of pipetting, and long hours of incubation [42,43]. ELISA is also susceptible to non-specific binding of the antigen or antibody to the surface of a plate, which can lead to false-positive results and low diagnostic specificity. Moreover, the synthesis of antibodies may be be challenging for some pathogens [40].

2.4. Lateral flow immunoassay (LFA)

LFA is the most widely used diagnostic technique in point-of-care (POC) settings (*e.g.* pregnancy dipstick tests) due to its simplicity, portability, and rapid response time. Since the introduction of the LFA assay in late 1960s for diagnosis of diseases, it has been used for the detection of many infections such as HIV, malaria, meningitis, flu viruses, gonorrhea, tuberculosis and rubella [23,44–47]. In LFA, the analyte travels along a polymeric strip with reporter probes by capillary force and encounters a detection zone, where the capture probes are immobilized. Binding of analyte-reporter complex to capture probes in the detection zone produces a visible line on the pad [48]. There are several variants of LFA to detect either proteomic or genomic biomarkers. The exclusive use of antibodies as recognition molecules is known as a lateral flow immunoassay, whereas the hybridization of nucleic acids with immobilized complementary strands is called nucleic acid LFA [48]. LFAs do not require washing steps, and can be performed in one-step, which significantly reduce the amount of sample handling. However, LFA has micromolar (μM) analytical sensitivity, and provides only qualitative or semi-quantitative results precluding its use for diagnosis of pathogens that are presented at low concentrations.

2.5. Polymerase chain reaction

PCR is used for the amplification of nucleic acids (either RNA or DNA) and many infectious diseases are diagnosed using PCR to determine the presence of genetic biomarkers. Several variants of PCR have been developed to serve different purposes including quantitative and digital PCR for measuring the amount of target nucleic acids, asymmetric PCR for generating single-stranded amplicons, reverse-transcription PCR for amplifying RNA, and multiplex PCR for amplifying multiple sequences simultaneously [49–54]. In all PCR reactions, a nucleic acid sequence is amplified through repetitive cycles of denaturation of double stranded sequence, hybridization with primers, and extension of primers with polymerase, producing a large amount of amplicons [55]. The detection of amplicons can be carried out *via* several methods such as gel electrophoresis, real-time fluorescence measurement, or sandwich hybridization assay.

PCR offers the highest sensitivity, and can detect as low as 5 to 10 nucleic acid copies [56]; however, it is not well suited for use in POC settings due to the need for an expensive thermocycler and trained technicians [57]. Recently, many groups have started to miniaturize PCR device with microfluidic technologies and chips for use in POC testing [58]. There are mainly two microfluidic PCR chip designs, which are the stationary reaction chamber and continuous flow systems. In the stationary reaction chamber system, the PCR mixture is kept stationary while the heating unit positioned underneath alternates its temperature. On the other hand, the continuous flow system contains pre-fixed temperature zones, where the PCR mixture flows. Although researchers have successfully miniaturized PCR systems using a microfluidic approach, it still requires complex and bulky peripherals. For instance, large gas tanks or syringe pumps are often used as the pressure source for fluid actuation, and bulky microscopes or electrical instruments are required for signal readout [58].

Furthermore, the ultrahigh sensitivity of PCR assay makes it prone to easy contamination by trace amounts of DNA, leading to false-positive results [59]. Nucleic acid based detection can also be problematic because it requires a complex sample preparation step. DNA and RNA generally do not float directly in blood or other bodily fluids, but need to be extracted from the pathogen [60]. This extraction step is further complicated for RNA samples, since RNA degrading enzymes, RNases, are present in most bodily fluids and cause rapid degradation of extracted RNA unless careful extraction protocol is followed. Finally, the genomes of some organisms, in particular viruses, are subject to high mutation rates, leading to high variability within their sequences [61]. Therefore in some cases, identification of conserved target regions that allow detection of pathogen variants becomes challenging.

3. Properties of nanomaterials

Nanomaterials have been extensively used in the development of various *in vitro* diagnostics due to their unique optical, magnetic, electrical, and thermal properties. These properties can be used to either generate different types of detection signals, amplify the intensity of the detection signals, or simplify diagnostic procedures. This section will discuss the properties of three nanomaterials (quantum dots, gold nanoparticles, and magnetic nanoparticles) that are commonly used in diagnostic applications. They represent the major developments in nanotechnology for infectious disease diagnostic systems.

3.1. Quantum dots (QDs)

QDs are semiconducting nanocrystals and composed of atoms from groups II-VI, IV-VI or III-V in the periodic table [62]. These nanomaterials exhibit quantum confinement effects, which lead to size-dependent electrical and optical properties [63]. In a bulk-scale semiconductor, the energy states are grouped into energy bands, where an electron from the valence band (*i.e.* highest occupied electronic state) gets excited to the conduction band (*i.e.* lowest unoccupied electronic state) upon the absorption of a photon, leaving a vacancy in the valence band (*i.e.* hole). The excited electron and remaining hole are attracted to each other by the electrostatic force, and this electron-hole pair is referred to as an exciton. As the size of a semiconducting material becomes near or smaller than the exciton Bohr radius (typically less than 100 nm), which is the case for QDs, the energy bands become discrete energy levels with potential barriers that confine the electron motion (Fig. 2A). This quantum confinement effect forms the basis of size-tunable properties of QDs. As the size of a QD increases, the discrete energy levels split and results in a narrower bandgap, which corresponds to the emission of a longer wavelength photon upon the recombination of an electron-hole pair (Fig. 2A). This allows the fluorescence emission of a QD to be tuned by manipulating their size to produce a variety of emission wavelengths (Fig. 2B).

Additionally, QDs present a broad and continuous absorption spectrum, which provides a large separation between the excitation and emission wavelengths (*i.e.* Stokes shift) compared to organic dyes (Fig. 2C) [64–66]. This optical property becomes useful for diagnostic applications because QDs of different emission profiles can all be excited using a single light source given that the energy of excitation is greater than the largest bandgap energy among QDs of different sizes. For instance, a light source with its wavelength in the ultraviolet (UV) range can excite all Cadmium Selenide (CdSe) QDs that emit fluorescence in the visible range as opposed to organic dyes that typically require multiple excitation sources for different emission profiles. Also, QDs have narrower emission spectra, better photostability and are brighter than organic dyes. For example, the emission spectrum of a QD is symmetric and can have a full width at half maximum (FWHM) as low as 12 nm [67], whereas an organic fluorophore is often characterized with an asymmetric emission spectrum tailing to the longer wavelength with its FWHM between 50 and 100 nm [68]. Such optical properties of QDs become useful for many bio-labeling and *in vitro* diagnostic applications [64–66].

3.2. Gold nanoparticles (GNPs)

GNPs are metallic nanostructures that have been used as early as in the 4th century BC for glass staining and making of the Lycurgus Cup by Romans [69]. GNPs display surface plasmon resonance effect, which contributes to their unique optical and thermal properties. When GNPs are irradiated by light, the oscillation of electric field causes synchronized oscillation of conduction band electrons, also known as the plasmons, as illustrated in Fig. 3A [70]. The displacement of conduction band electrons then creates a net charge difference or a dipole on the surface. Such induced dipole that oscillates in-phase with the electric field of the incident light causes a strong absorption of light at specific wavelengths [71]. For sub-50 nm spherical GNPs, light gets absorbed near the wavelengths of blue and green colors, and transmitted with the wavelength of a red color (Fig. 3B). A solution of small spherical GNPs therefore appears as a red color. The oscillation frequency or the absorption wavelength depends on the electron density, the effective mass of the electron, and the charge distribution, which can all be influenced by the size, shape and surface chemistry of the particles [70]. As the size of GNPs increases, the absorption peak becomes shifted to a longer wavelength, and the solution becomes a dark purple color (Fig. 3B). As opposed to spherical GNPs that have a single absorption peak, gold nanorods have two absorption peaks: one in the visible range that corresponds to the transverse plasmon, and another in the near infrared range, which corresponds to the longitudinal plasmon [20,72] (Fig. 3C). The inter-particle spacing also affects the absorption profile of GNPs. When the inter-particle distance becomes smaller than the diameter of GNPs, the solution color changes from red to purple or blue depending on the extent of aggregation due to the coupling of surface plasmons that shifts the absorbance peak to a longer wavelength (Fig. 3D) [73].

GNPs can also generate heat upon light exposure. When the frequency of incident light matches the surface plasmon resonance absorption peak, GNPs can produce heat *via* non-radiative decay. In this process, the excited hot electrons transfer their energy to the lattice upon relaxation. This process is followed by a phonon-phonon interaction in which the lattice energy is dissipated to the surrounding medium resulting in local heating around nanoparticles [20,74].

3.3. Magnetic nanoparticles (MNPs)

Several types of MNPs exist including cobalt oxide, nickel oxide and iron oxide nanoparticles. Out of these, iron oxide nanoparticles are the most extensively explored MNPs in biomedicine due to their biocompatibility, biodegradability, and superparamagnetic properties [19,75]. In the macroscale, electrons of the magnetic particles can either spin in the opposite or same directions, in which the opposing spins cancel each other out, and weaken the localized magnetic field. On the other hand, magnetic particles at the nanoscale have more constrained electrons that only spin in the same direction, which strengthen the localized magnetic field [19]. For example, superparamagnetic iron oxide nanoparticles (SPIONs) that are smaller than 20 nm have a single domain of electrons that spin in the same direction, whereas iron oxide macroparticles that are greater than 20 nm have multiple domains of electrons with opposite spins (Fig. 4) [19]. Hence, SPIONs reveal much greater magnetic susceptibility to external magnetic field when compared to paramagnetic materials. Unlike ferromagnetic materials that remain magnetized permanently, SPIONs can get demagnetized with the removal of the external magnetic field. For these reasons, there are some Food and Drug Administration (FDA) approved MNPs that are currently being used as contrast agents in Magnetic Resonance Imaging (MRI) [76], and many companies sell MNPs for isolation of cells or extraction of biological molecules such as proteins and nucleic acids.

4. Various detection modalities of nanodiagnostics

In the last two decades, large amount of research has been

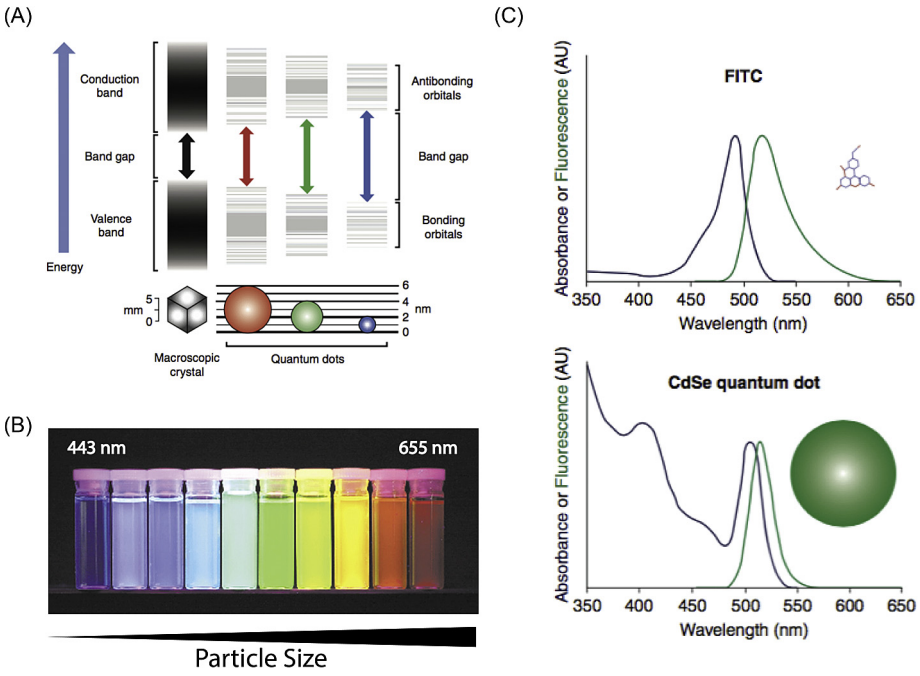

Fig. 2. Optical Properties of QDs. (A) Discrete energy levels of QDs compared to continuous energy states (i.e. energy bands) in a macroscopic semiconductor, and the size-dependent bandgap energies of QDs. Figure adapted from source [179]. Copyright (2010) Dimitris Ioannou and Darren K. Griffin. (B) CdSe-ZnS (core-shell) QDs excited with a near-UV lamp showing emission peaks at 443, 473, 481, 500, 518, 543, 565, 587, 610, and 655 nm (from blue to red). Figure adapted from source [84]. Copyright (2001) Nature Publishing Group. (C) Absorption and emission spectra of an organic dye (fluorescein isothiocyanate, i.e. FITC), and QD (CdSe). Figure adapted from source [179]. Copyright (2010) Dimitris Ioannou and Darren K. Griffin.

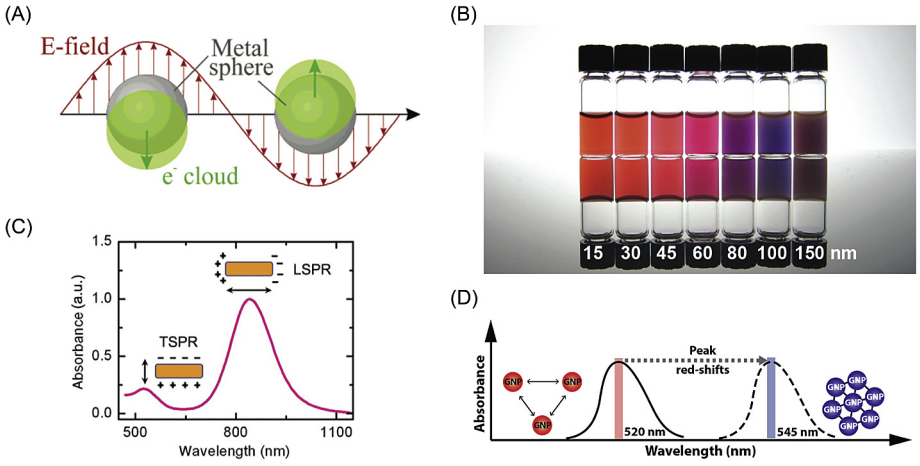

Fig. 3. Optical Properties of GNPs. (A) Surface plasmon resonance of spherical GNPs showing the synchronized oscillation of conduction band electrons relative to the electric field of incident light. Figure adapted from source [70]. Copyright (2003) American Chemical Society. (B) Size-dependent optical property of GNPs. As the diameter increases (15–150 nm), the peak absorbance wavelength shifts to a longer wavelength, resulting in a darker solution color. Image courtesy of Abdullah Muhammed Syed. (C) Absorption profile of gold nanorods with two distinct peaks that correspond to transverse and longitudinal plasmons. Figure adapted from source [180]. Copyright (2013) Chinese Laser Press. (D) Coupling of surface plasmons. Aggregation of GNPs shifts the absorption peak to a longer wavelength. (For interpretation of the references to colour in this figure legend, the reader is referred to the web version of this article.)

conducted to apply advances in nanotechnology to diagnosis of infectious diseases. Unique properties of nanoparticles have been used to both improve detection capability of traditional molecular assays, and to develop completely novel methodologies. This section outlines various approaches of using nanoparticles for different detection modalities (fluorescence, surface-enhanced Raman, magnetic, electrochemical, colorimetric, and thermal). This discussion is summarized in Table 1, and the comparison of analytical sensitivities in relation to conventional diagnostic methods is illustrated in Fig. 11.

4.1. Fluorescence-based biosensors using nanoparticles

Fluorescence-based techniques are commonly used for detection of nucleic acid and protein targets. However, conventional fluorophores suffer from photobleaching, low quantum yield, wide emission spectra that limit multiplexing capabilities, and narrow absorption spectra that require multiple excitation sources. Therefore, QDs have been extensively used to address limitations of traditional organic fluorophores.

For instance, QDs have been used as reporter labels for sandwich

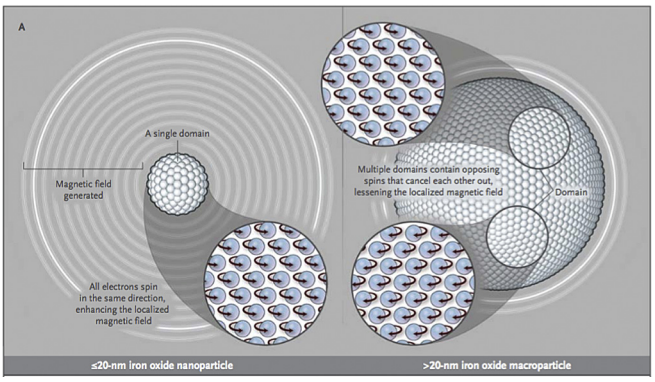

Fig. 4. Size-dependent Properties of Iron Oxide MNPs. Figure adapted from source [19]. Copyright (2010) Massachusetts Medical Society.

ELISA-type immuno-assays and DNA microarrays in a singleplex or multiplex format for detection of chemical residues and cancer antigens [77–80] (Fig. 5A and B). In one study, Park et al. adopted a typical sandwich immuno-assay with the addition of surface-engineered QDs, which were used as signal amplifiable reporter labels. The self-assembly of QDs was designed using streptavidin-biotin conjugate pair and zwitterionic surface modification. In this system, myoglobin first binds to immobilized capture antibody, followed by binding of myoglobin detection antibody and biotinylated secondary detection antibody. This is then followed by the binding of streptavidin conjugated QDs, which will then bind to biotin conjugated QDs in a layer-by-layer approach (Fig. 5B). This system demonstrated detection of myoglobin with sub-attomolar limit of detection (LOD) [80]. QDs have also been used in the context of engineering Förster Resonance Energy Transfer (FRET) based detection systems [81–83], and multiplexed diagnostics [84–86]. FRET based assays utilize QDs as energy donors, which transfer the energy to acceptor fluorophores or quenchers for detection of small molecules and nucleic acids. This allowed for the sensitive detection of DNA (10 pM–1 nM LOD, [87,88]) and small molecules (1 nM–1 μM LOD, [89,90]).

The multiplexing capability of QDs can be illustrated by the development of barcodes. Different combinations of QDs can be infused into polymeric microbeads to generate fluorescent barcodes (Fig. 5C). The surface of the QD encoded microbeads can be functionalized with DNA capture probes, which hybridize with the target DNA labeled with a fluorescent dye, yielding both the barcode and detection signals [84]. In this complex, the barcode signal can be used to determine the identity of a target DNA (*e.g.* the type of an infectious disease, genotype or subtype of a disease, antibiotic resistance, *etc.*), and the detection signal can be used to determine the presence or the absence of a target DNA (*i.e.* whether a patient is infected or not). These QD barcodes can be designed with different colors (m) and intensity levels (n) to generate (n^m-1) barcode signals [84]. For instance, combinations of 6 QD colors with 10 intensity levels can theoretically create one million barcodes [84]. Although the actual multiplexing capacity would be much lower due to the requirement of signal-to-noise ratio, spectral overlaps, and variations in the fluorescence intensity [84], QD barcodes opened up a new opportunity to further improve multiplexed diagnosis and high-throughput screening of infectious diseases. Previously, a library of over 100 barcode signals was generated with 2 QD colors from a set of 5, at 2 intensity ratios *via* concentration-controlled flow-focusing (CCFF) method, which demonstrated a highly robust way of synthesizing optically encoded microbeads that are stable at a wide range of biological environments (*e.g.* temperature, pH, and buffer conditions) with good monodispersity [91] (Fig. 5C).

Table 1
Comparison of nanodiagnostics.

Technology	Implementations	Targets	LOD Range	Advantages	Limitations
Fluorescence	Bead encapsulated dye and QD, QD labels, GNP-QD quench pairs, QD-Dye FRET	• Nucleic acids • Proteins • Small molecules • Bacteria • Viruses	0.8 pM–12 nM 40 fM–1 nM 100 pM–1 μM Single cell 0.1 PFU/mL	Optimal for multiplexing, good sensitivity	Need for readout equipment
Surface enhanced Raman spectroscopy (SERS)	Metallic nanoparticles in solution/on surface, active tip, patterned nanostructures	• Nucleic acids • Proteins • Bacteria • Viruses	10 pM–100 nM 30 fM–100 pM 250 CFU/mL 100 PFU/mL	Best for multiplexing, potential for extremely high sensitivity	POC setup not compatible with high sensitivity, expensive readout equipment
Magnetic	Magnetic separation Assays based on magnetic NMR readout	• Nucleic acids • Proteins • Nucleic acids • Proteins • Bacteria	500 zM 30 aM–0.5 pM 0.2 pM–10 pM 1 pM 1000 CFU/mL	Very high sensitivity Good sensitivity	Complex multi-step reactions Need for readout equipment
Electrochemical	Biocatalytic or affinity format, GNPs and CNTs electrode coating, nanoparticle labels	• Nucleic acids • Proteins • Small molecules • Bacteria • Viruses	aM–fM fM–nM pM–μM 10–100 cells Single virus	Good sensitivity, simple readout electronics	Non-specific adsorption, need for pH control
Colorimetric	Color change associated with GNP aggregation	• Nucleic acids • Proteins • Small molecules	1 pM–μM 4.4 pM–μM 1 nM–1 μM	No need for readout equipment	Limited sensitivity
Thermal	Temperature change after excitation of GNPs with a laser in a lateral flow immunoassay	• Proteins	2.7 pM	Good sensitivity	Need for readout equipment

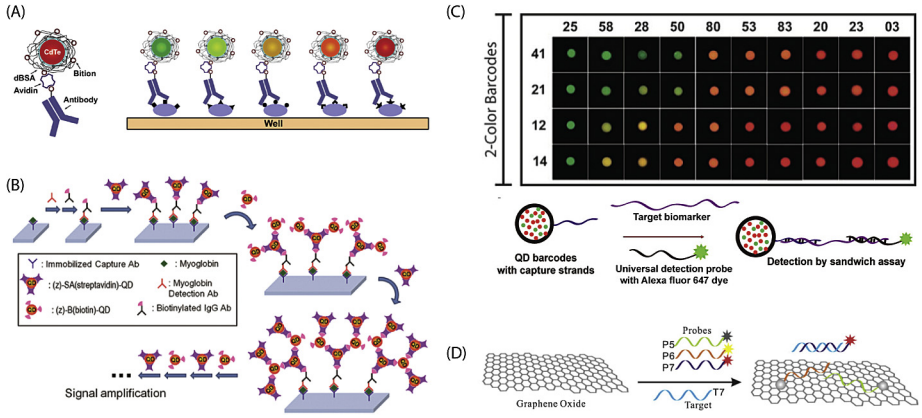

Fig. 5. Examples of Fluorescence-based Biosensors using Nanoparticle. Images are adapted from indicated references. (A) QDs can be used as labels in multiplex ELISA [79]. (B) Signal amplifiable reporter labels using self-assembly of QDs. Self-assembly is achieved *via* streptavidin-biotin interaction [80]. (C) Controlling ratio of green/red QDs encapsulated into polymer beads to make over 100 unique barcodes; QD barcodes can detect analytes in multiplex format [86,91]. (D) Fluorescently functionalized ssDNA adsorption onto graphene quenches fluorescence; in the presence of complementary target dsDNA remains resuspended; can be performed in multiplex with different dyes [106].

Additionally, high-throughput synthesis of QD barcodes was demonstrated using a combined membrane emulsification-solvent evaporation approach [92]. Studies have also shown multiplexed detection of several genomic and proteomic biomarkers for infectious diseases such as HIV, HBV, HCV, malaria, and syphilis using QD barcodes in a sandwich assay format with pM sensitivity [85,86]. Moreover, coating the surface of QD barcodes with metal nanoshells was shown to improve the analytical sensitivity of the assay by 2-orders of magnitude due to the metal-enhanced fluorescence effect, and achieve better bead stability, fluorescence consistency and loading capacity of recognition molecules [93]. More recently, QD barcode assay was clinically validated to achieve high clinical sensitivity (~90%) and specificity (~95%) by detecting multiple regions of HBV genome [94]. Such multiplexing capability of QD barcodes is useful in the development of diagnostics because it can reduce labor cost and time involved in the detection of multiple biomarkers.

GNPs exhibit surface plasmon resonance (SPR) effect, which have been used for quenching emission from fluorescent dyes that are positioned close to the surface [95,96]. This quenching can act over long distances (as large as 75 nm [97]), and depends on particle shape [98,99] and size [95,100]. Therefore, GNPs have been adapted for FRET assays, in which the energy state associated with the excited electron is non-radiatively transferred from the fluorophore to the nanoparticle. This assay format demonstrated improved detection sensitivity [101], better selectivity to single base mismatches [102] and simultaneous quenching of multiple dyes [103]. In addition, GNP-QD molecular systems have been reported where QDs are efficiently quenched by the GNPs. These constructs have been used to quantify viral titer in living cells down to 0.1 PFU/mL [104] and to detect influenza antigen (hemagglutinin) with ~100 pM sensitivity [105]. Similarly to GNPs, graphene oxide can also quench fluorophores or QDs attached to its surface [106–109]. As illustrated in Fig. 5D, graphene oxide can bind to dye-labeled single-stranded DNA probes and quench fluorescent signals in the absence of target DNA, whereas the formation of a duplex with its target releases the DNA from graphene oxide and recovers fluorescence signal.

4.2. Surface-enhanced Raman spectroscopy (SERS) using nanoparticles

Raman spectroscopy is a technique used to observe contributions of rotational and vibrational energy states of molecules to the absorbance spectrum of the material. SPR effect of plasmonic nanoparticles has been used to greatly enhance the signal from Raman spectroscopy. For instance, GNPs coated with Ramen reporter molecules have been used for detection of surface envelope and capsid antigens of West Nile and Rift Valley fever viruses (Fig. 6A). The presence of the antigen links MNPs with GNP reporter probes, which become magnetically separated, and GNPs enhance SERS signal emitted from Raman reporter molecules. DNA detection has been also demonstrated, which involved hybridization between TAMRA (TMR) labeled target DNA and capture probe functionalized GNPs (Fig. 6B). This hybridization brings TMR in close proximity with GNP, and enhanced TMR Raman signature. Similarly, Raman dye labeled oligonucleotide probes have been conjugated to GNPs in a scanometric assay to generate spectroscopic codes for individual target DNA and demonstrate a multiplexed detection (Fig. 6C). In this system, the presence of target DNA connects GNP probes with capture DNA attached on a planar surface. Silver staining of GNPs determines the presence of the target, and the identity of the target is revealed by SERS signals.

Since Raman profile consists of multiple element-specific absorption spectrum features, which can be as narrow as 1 nm FWHM [110], this technique allows for high degree of multiplexing [111,112]. However, the major limitation is that traditional Raman scattering is associated with a low absorption cross-section, greatly limiting the detection sensitivity [113]. The signal can be significantly enhanced (as much as 10^{11} times [114]) when the molecule is positioned close to the surface of plasmonic nanoparticle, or in a "hot spot" created by the intersection of SPR fields of two or more nanoparticles, allowing for highly sensitive single-molecule detection [115]. In addition, the area under the absorption peaks scales with concentration, which can be used to quantify the amount of target analytes.

The generation of strong "hot spot" nonetheless requires precise geometry that is difficult to manufacture and which can erode over time. Furthermore, the distance of the SERS probe to the "hot spot" is critical, with the signal enhancement dropping by orders of magnitude even at a separation of a few nanometers. This generally results in variability of enhancement between different probes, which complicates analyte quantification [113]. Due to these considerations, most applications are based on less sensitive bulk rather than single-molecule nanoparticle systems, where SERS is achieved due to probe immobilization on metal nanoparticles in the solution phase. This technique has been successfully applied for detection of nucleic acids (10 pM–100 nM LOD) [116,117], proteins

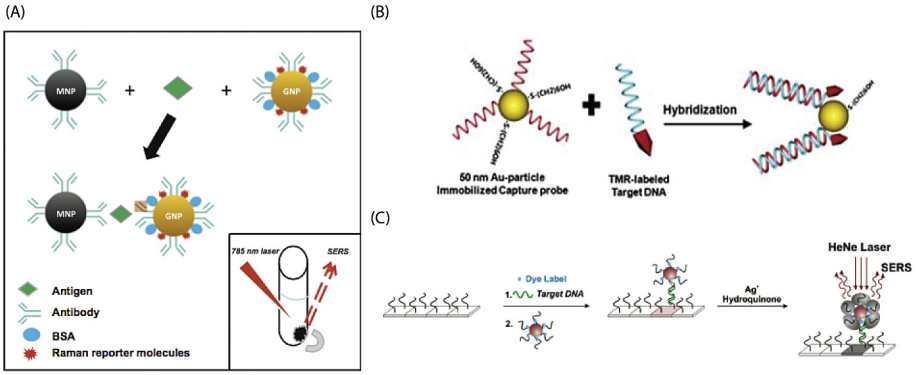

Fig. 6. Examples of SERS using Nanoparticles. Images are adapted from indicated references. (A) Antigen can link MNPs and GNPs. MNPs are used for magnetic separation and GNPs enhance SERS signal of the dye [123]. (B) Hybridization of the dye-labeled DNA to GNP-immobilized strand increases SERS signal [113]. (C) Scanometric assay can be used with SERS readout [138].

(100 pM LOD) [118], cancer cells [119], bacteria (250 cells/mL LOD) [120,121] and viruses (100 PFU/mL LOD) [122,123], and for tracking small molecule drugs inside living cells (100 pM LOD) [124]. One major drawback of this technique is that the probe must be positioned close to the nanoparticle surface, which limits the choice of nanoparticle surface chemistry. Another limitation is that SERS requires high power lasers for excitation and expensive equipment for readout. This complicates the translation of this technique to POC applications.

4.3. Magnetic nanoparticles (MNPs) for biosensing

MNPs have been explored in the development of many biosensing assays because they allow for the separation of reagents in a magnetic field. The use of MNPs in assays can simplify the design of the diagnostics that include separation or washing steps. For example, a conventional QD barcode assay has been automated with the additional encoding of the barcodes with MNPs and using permanent magnets in a microfluidic device (Fig. 7A). The microfluidic device was designed to magnetically move the barcodes to a stream containing target DNA, move back to a stream containing reporter probes, and finally immobilize the barcodes during the washing of excess reporter probes [125]. The use of magnetism simplified the entire assay process.

Magnetic separation was also implemented in a highly sensitive bio-barcode assay developed by Mirkin and Letsinger groups [126] (Fig. 7B). This design combines MNPs with gold reporter nanoparticles, both functionalized on their surface with a ligand (which can be DNA or antibody) designed to recognize and bind to the analytical target. Binding of analyte crosslinks the two particles, allowing the GNPs to be magnetically separated together with the MNPs. Barcode DNA is then released from GNPs, and detected *via* scanometric assay. In the scanometric assay, barcode DNA connects GNPs with capture probes that are attached on a planar substrate, followed by silver staining of bound GNPs. This system contains two levels of signal amplification. The release of barcode DNA from GNPs initiates the first amplification, and the subsequent silver staining of GNPs gives rise to the second amplification. Thus, application of this assay has produced ultrasensitive detection of proteins (500 aM [127]), and DNA (500 zM [126]), where detection limit of DNA is comparable to that achieved with quantitative PCR. However, this assay is complex, requires multiple steps, and takes approximately 6 hours to complete.

MNPs can also be directly used as reporter probes to generate magnetic signals that correspond to the presence of target molecules. For instance, the transverse relaxation time (T_2) of a sample can be altered and measured using a micro Nuclear Magnetic Resonance (μNMR) device by either decorating the surface of the microbeads with MNPs in the presence of the target DNA [128,129] (Fig. 7C), tagging the surface of target cells with MNPs [130], or by aggregating MNPs in the presence of target analytes [131]. Reported results included detection of proteins with 1 pM LOD [132], nucleic acids at concentrations as low as 0.2–10 pM [133,134], and identification of as few as 2 cancer cells [135] and 1 CFU of bacteria [131] in 1 μL of sample.

4.4. Electrochemical (EC) biosensors using nanoparticles

EC assays are another group of biosensors that have been developed over the last 50 years. These sensors are based on the premise that interaction with the chemical analyte changes one of the electrical properties of the system: current, potential, or impedance, which can be recorded by an electronic device. Two main sensing schemes are (i) biocatalytic and (ii) affinity biosensors [136]. In the biocatalytic scheme, enzyme whose substrate is the target analyte is immobilized on the electrode's surface. Upon analyte binding, the enzyme either produces electrically active chemical species, or directly transfers electrons to the electrode. High catalytic activity of enzymes results in high sensitivity (fM, [137]) and specificity of substrate binding allows the detection to be performed in complex mixtures without sample pre-processing. However, a major limitation is that enzymes are only available for a limited number of substrates. Affinity-based detection is an alternative EC technique in which electrodes are coated either with antibodies or DNA probes designed to recognize target protein or small molecule antigen, or to hybridize to the complementary DNA. Binding of the target to these probes modulates the electronic properties of the surface, and results in changes in the recorded signal. Since antibodies for a large number of antigens are available and DNA probes can be designed for any sequence, this technique has been extended to much larger number of analytes. However, a lack of amplification step limits the sensitivity of EC affinity biosensors.

Several nanoparticle-based approaches have been developed to improve the sensitivity of affinity EC biosensors. In one study, nanowire field effect transistors have been modified with different antibody receptors for detection of single virus particles (Fig. 8A). Binding of a single virus to one of the nanowires changed the conductance, which is a characteristic of the viral surface charge that is only unique to that nanowire. The conductance was returned to the baseline value once the virus unbinds from the nanowire. Scanometric assay has also been used in an EC biosensor (Fig. 8B).

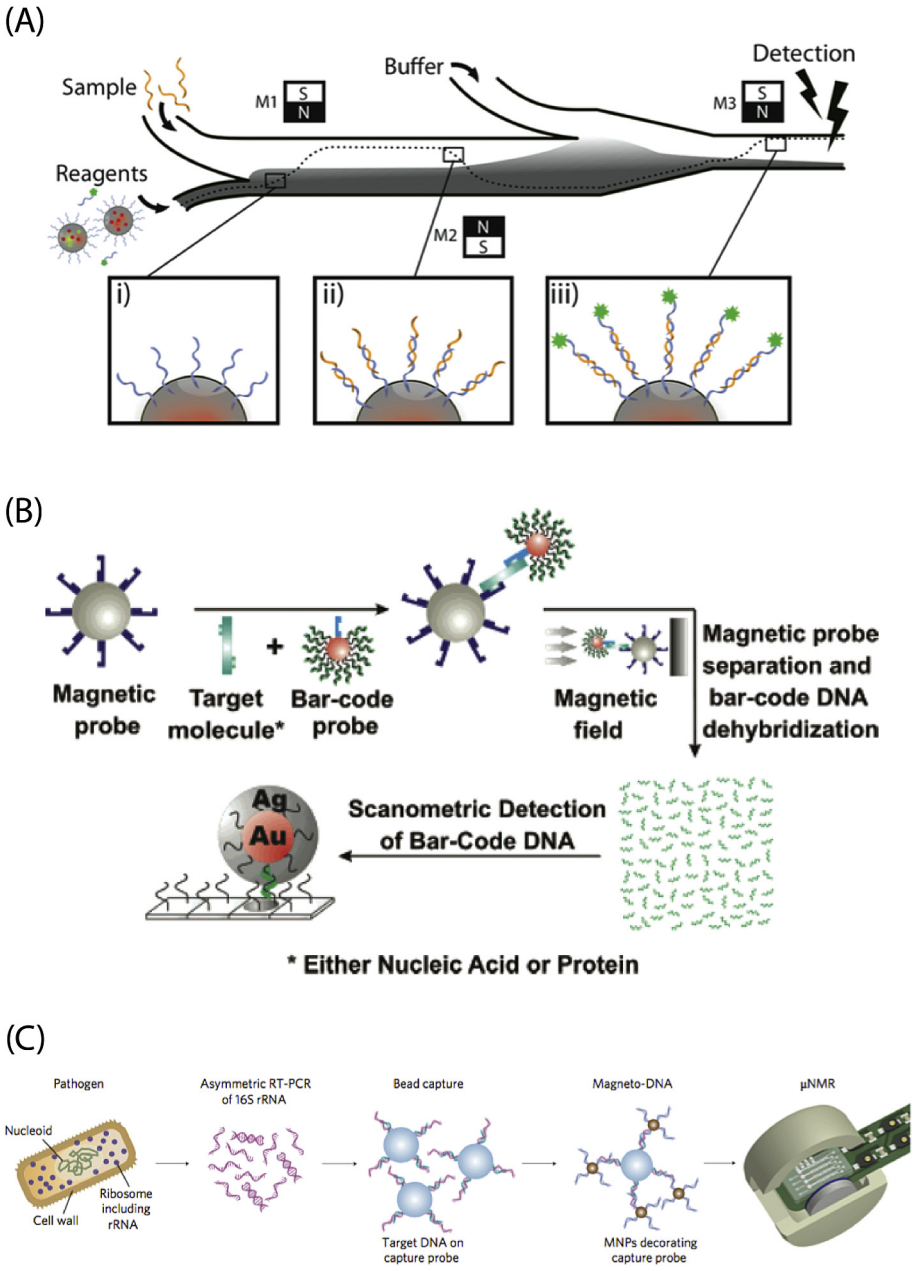

Fig. 7. Examples of using Magnetic Nanoparticles for Biosensing. Images are adapted from indicated references. (A) QD barcode assay automated by encoding microbeads with MNPs and using a microfluidic device [125]. (B) Highly sensitive scanometric assay developed by Mirkin group [138]; MNPs are used for magnetic separation. (C) Presence of target DNA links MNPs to a bead surface; this affects their magnetic momentum, which can be detected with a portable μNMR device developed by Weissleder group [128].

In this system, capture probes are immobilized in the gap between two electrodes, followed by the sandwich hybridization of capture, target and GNP DNA probes. Catalytic reduction of the silver allows current to flow between two electrodes, whereas in the absence of the target DNA, there is no current flow.

The electrodes can also be coated with GNPs or carbon nanotubes, both of which affect impedance resulting in higher sensitivity (Fig. 8C). Reported results include detection of DNA (pM LOD [138–142]), proteins (1 nM LOD [143]), single viruses [144] and 10 to 100 bacteria [145]. Another approach uses nanoparticles to label surface-bound analytes in a sandwich-like format, which increases the sensitivity of detection by enhancing the strength of impedance modulation. This assay format was used to detect nucleic acids (fM LOD [146,147]), and proteins (fM LOD [148]). Multiplex detection of DNA was also reported using labeling with four different nanocrystals with distinct voltammetric signatures [149]. Limitations of EC assays include non-specific adsorption, the need to control ionic strength of the test solution and their relatively short shelf-life [150].

4.5. Colorimetric assays using nanoparticles

Colorimetric assays are advantageous over other assay formats because they do not require any equipment for readout and therefore are optimally suited for POC applications. The most widely reported format, which is based on aggregation of GNPs, was developed by Mirkin and coworkers [151,152]. Due to the SPR effect, GNPs show strong absorbance in visible wavelengths. For

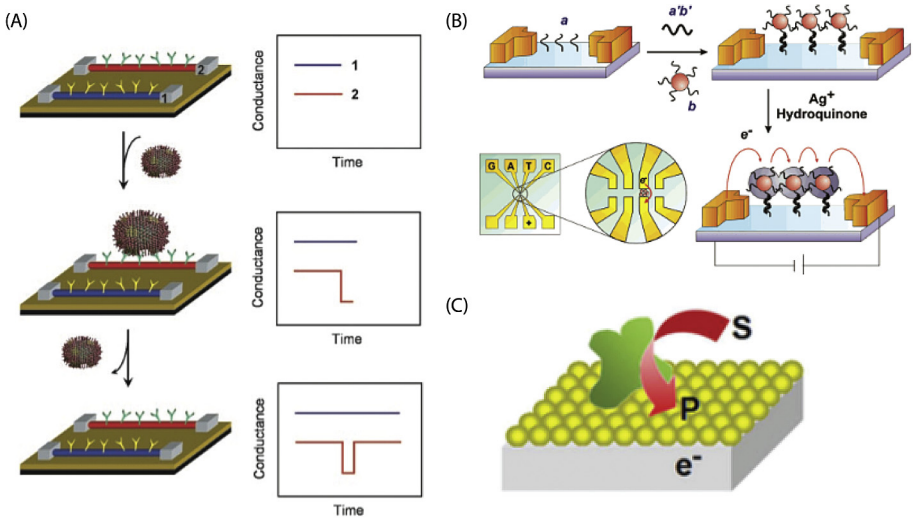

Fig. 8. Examples of Electrochemical Bionsensors using Nanoparticles. Images are adapted from indicated references. (A) Nanowire electrodes allow detection of singe viral particles [144]. (B) EC signal is an alternative readout for the scanometric assay shown in Fig. 7A [138]. (C) Electrode coating with GNPs enhances electron production due to faster redox process [181].

13 nm GNPs, which are generally used for these assays, the absorption wavelength is 520 nm, making the solution of these nanoparticles appear brightly red. However, if nanoparticles are brought together in close proximity (*i.e.* when inter-particle spacing becomes smaller than diameter of GNPs), their SPR fields couple and resonance peak shifts to longer wavelengths, which results in red-to-blue color transition that is easily visible by a naked eye. Several implementations have been reported where binding of the analyte causes either aggregation or dispersion of GNPs for colorimetric detection of IDs (Fig. 9A).

The simplest form of colorimetric assay has been demonstrated with detection of nucleic acids using either a one probe or two probes strategies [153]. In the one probe strategy, the surface of GNPs is functionalized with one type of DNA probe that is complementary to target DNA. In the presence of target DNA, GNPs remain monodispersed due to hybridization of target DNA with GNP probes, which stabilizes GNPs and prevent aggregation by salts. On the other hand, in the absence of target DNA, GNP aggregation is induced by high salt concentration, which causes a color change from red to blue [154,155]. In the two probes strategy, two sets of GNPs are prepared with different probes. The presence of target DNA crosslinks two sets of GNPs and cause aggregation, whereas in the absence of target DNA, two sets of GNPs remain monodispersed in a solution [156,157].

Besides detection of DNA, novel modifications and introduction of functional nucleic acid molecules, such as aptamers or DNAzymes, allowed the assay to be extended to detect small molecules, metal ions, proteins, and bacterial cells [153,158–161]. For example, aptamer conjugated GNPs (*i.e.* aptasensors) have been used to detect *Escherichia coli* and *Salmonella typhimurium* (Fig. 9B). In this system, aptamers that are specifically designed to bind target bacteria are initially adsorbed on to the surface of GNPs, and prevented salt-induced aggregation due to electrostatic repulsion. The presence of the target bacteria changes the conformation of the aptamers, which results in the desorption of the aptamers from surface of GNPs, and results in the salt-induced aggregation of GNPs.

While GNP aggregation assays are simple, fast, and do not require any expensive equipment, one significant drawback is that they do not include any amplification steps, which limits their sensitivity to low nM range. Integrating plasmon coupling of GNPs with DNAzyme was studied to provide a linear amplification step and improve the sensitivity level in the detection of dengue virus nucleic acid. This system consists of DNAzyme attached to the surface of 15 nm GNPs, where DNAzyme gets triggered by the addition of magnesium ions for cleavage of viral RNA, and cleaved RNA induce aggregation of GNPs in the presence of salt and heat [162]. Another example includes the integration of the plasmon coupling of GNPs with multicomponent nucleic acid enzyme (MNAzyme) [163,164] (Fig. 9C). This system consists of a set of GNPs aggregated by intact linker DNA, and MNAzyme components that are activated in the presence of target DNA to cleave the linker DNA, re-distributing GNPs to a monodispersed state. The switch of GNPs from aggregated to monodispersed state shifts the absorbance peak to a shorter wavelength, and correspondingly alters the solution color from dark purple to red. Hence, MNAzyme-GNP assay can provide a simple and fast colorimetric detection of genetic targets for POC diagnosis of infectious pathogens; however, there is still a need for an additional signal amplification strategy to detect pathogens that are presented at low concentrations.

4.6. Thermometry-based biosensors using nanoparticles

Heat-producing nanoparticles have been classically demonstrated in hyperthermia therapy of cancerous tissues [165–168]. Recent studies have started to exploit the thermal properties of metal nanoparticles for diagnosis of infectious diseases. Many types of nanoparticles can generate heat upon optical or electrical excitation. For example, both gold nanoshells and carbon nanotubes can produce thermal emission upon excitation in the near-infrared wavelength. The electrons of these excited nanoparticles interact with localized water molecules to induce vibration and dissipate heat when they transition to the ground state [169]. Nanoparticles that are poor fluorophores (*i.e.* low quantum yield) can generate a significant amount of thermal energy or heat. Recently, Bischof and co-workers demonstrated the use of thermal imaging to detect gold nanoparticles in lateral flow immunoassays (Fig. 10A and B) [170,171]. In this system, antibody-labeled GNPs were used as a contrast agent in conjunction with a thermal contrast amplification reader. The thermal contrast amplification reader matched the

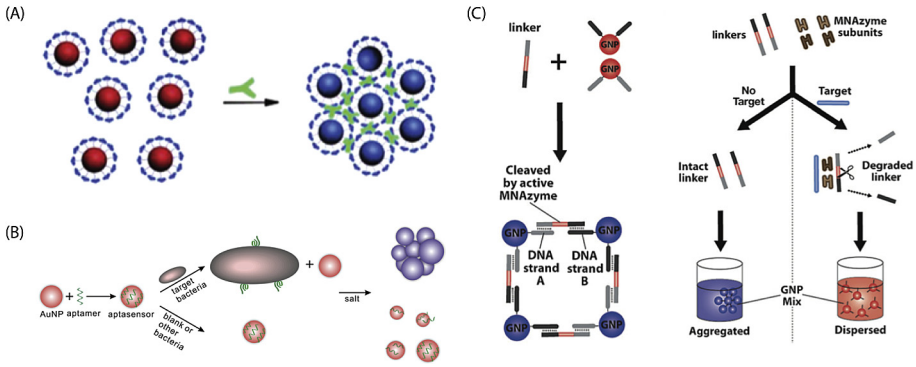

Fig. 9. Colorimetric Assays using Nanoparticles. Images are adapted from indicated references. (A) Antibodies can aggregate GNPs into microassemblies; nanoparticles turn purple due to surface plasmon resonance coupling [182]. (B) Aptasensor detects bacteria. The presence of target bacteria causes desorption of aptamers from GNPs, which also induces aggregation of GNPs in the presence of high salt concentrations [161]. (C) MNAzyme-GNP assay. Intact linker DNA induces aggregation of GNPs. The presence of target DNA activates MNAzyme components, which cleave linker DNA, and re-distribute GNPs to a monodispersed state.

laser wavelength to the GNP plasmon resonance peak, and detected temperature rise using an infrared detector, allowing quantification of GNP signals.

Using thermal contrast led to a 32-fold improvement in the analytical sensitivity of detecting cryptococcal antigen [170]. When combined with a thermal contrast amplification reader, this group showed an 8-fold improvement in the analytical sensitivity of detecting influenza A, malaria, and Clostridium difficile in comparison to visual analysis of the lateral flow strip [171]. While this technology is still early in development, these results show that thermal contrast may enhance the analytical sensitivity to enable detection of infectious pathogens, which are normally done with more complex molecular diagnostics. This approach maintains the simplicity of lateral flow immunoassays, while providing higher analytical sensitivity.

4.7. Comparison of analytical sensitivities

As discussed previously, some nanoparticle-based assays were specifically designed to demonstrate the potential of improving analytical sensitivity of conventional diagnostic approaches. The comparison of the analytical sensitivities of nanodiagnostics with conventional diagnostic methods, namely ELISA and LFA for protein detection, and PCR for nucleic acid detection, is illustrated in Fig. 11. Colorimetric nanodiagnostic modality was able to demonstrate improvement in the analytical sensitivity (μM-pM) in comparison to LFA technique (μM), but still needs improvement to meet the analytical sensitivity of ELISA (nM-fM) for protein detection. However, other nanodiagnostic modalities (*i.e.* fluorescence, SERS, magnetic, electrochemical and thermal) demonstrated better and similar analytical sensitivities than LFA and ELISA respectively. For detection of nucleic acids, none of the nanodiagnostic approaches were as sensitive as PCR (zM), except for the Mirkin's bio-barcode assay that utilized magnetic separation, and two levels of signal amplification. Thus, there is a need to focus on improving the analytical sensitivity of nanoparticle-based diagnostic devices as the sensitivity may limit their utility in detection of patient samples.

5. Clinical successes of nanodiagnostics and future work

There are only a few notable nanodiagnostic systems that have successfully translated into clinical use from academic concept. The development of nanodiagnostics can be categorized into four stages as illustrated in Fig. 12A. The first stage was heavily focused on material characterization, where the researchers explored different methods to synthesize and purify nanomaterials, obtain good monodispersity and colloidal stability, and functionalize surface with various chemistries. This led to the pre-clinical development stage, which has been the main research work over the last decades. This stage involved determining analytical characteristics such as LODs and linear dynamic ranges using synthetic targets. The field is now moving beyond this demonstration phase and starting to focus on clinical validation of the diagnostic devices. During this transition phase, additional metrics that describe the accuracy of a diagnostic test will be used to evaluate the diagnostic technology. In evaluating the clinical performance of a diagnostic device, metrics such as clinical sensitivity and specificity, positive and negative predictive values, likelihood ratios, receiver operating characteristic curves (ROC), and diagnostic odds ratio, will be required (Table 2) [172]. The successful completion of clinical validation will confirm the intended diagnostic application of a system, such as screening, sub-typing, monitoring, quantifying or profiling drug resistance (Fig. 12B).

Once the clinical validation of nanodiagnostics is achieved, the next step is to conduct field testing within various operational contexts. Field testing of nanodiagnostics has been limited primarily due to the lack of an all-in-one device that can automate complex diagnostic procedures. Many nanodiagnostic systems involve extensive pipetting and laboratory work for extraction, amplification and detection of disease biomarkers, which significantly hamper their usage in the remote regions. This challenge needs to be addressed in the future by minimizing user interventions in the diagnostic procedure and replacing the bulky readout systems with a portable device. Chan's group proposed such system in 2015, which contains different compartments that are connected by capillary tubes for extraction, amplification, and detection of nucleic acids. The flow of reagents between compartments were proposed to be electrically driven, and this device will attach to a smartphone for measurement of final assay signals [173]. Another system was developed by Sia's group, who built a smartphone accessory that can run ELISA in a microfluidic format, and report the optical density of silver stained GNPs using a smartphone device [174]. Instead of using power-consuming electrical pump, this "dongle" utilized a rubber bulb that can be pressed to mechanically activate a negative pressure chamber and drive the flow of reagents that are stored in a microfluidic cassette. Other components in the dongle included light emitting diodes, photodetectors microcontroller, and an audio jack connector that can transmit data to the smartphone *via* frequency shift keying [174].

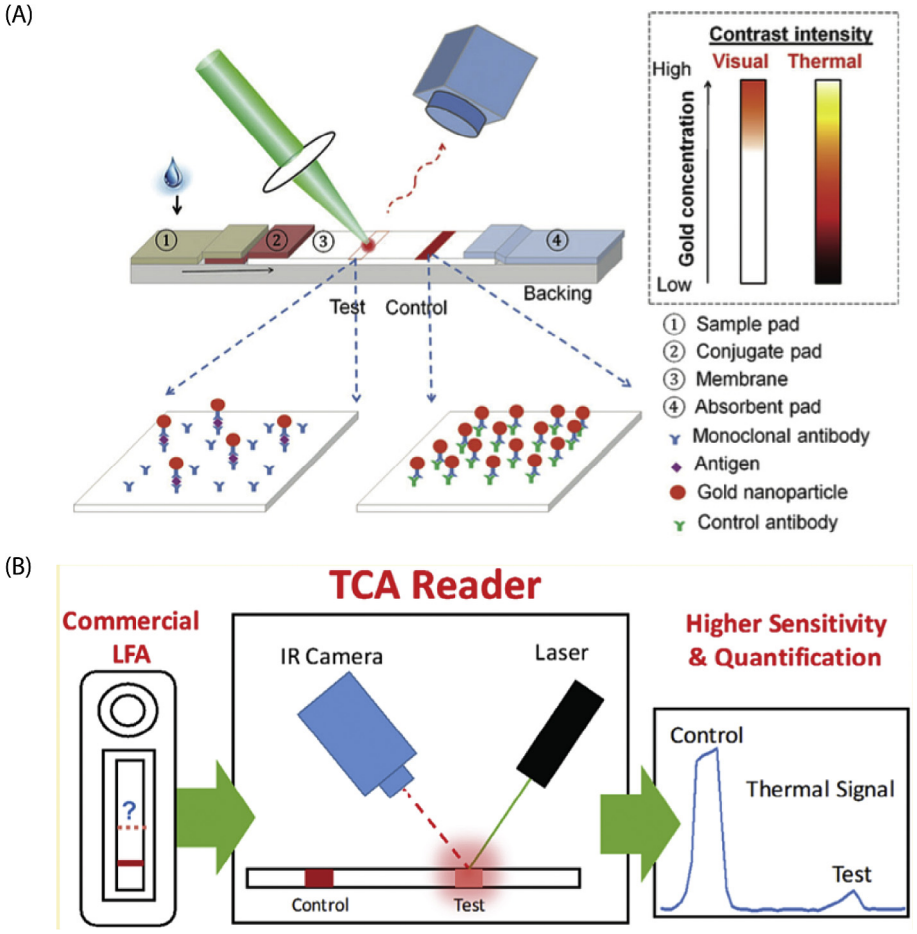

Fig. 10. Thermometry-based Biosensors using Nanoparticles. Images are adapted from indicated references. (A) GNPs are irradiated by a laser on a lateral flow immunoassay, and temperature change is recorded with an infrared camera. (B) Temperature Contrast Amplification (TCA) reader developed by Bischof group can thereby improve analytical sensitivity of conventional lateral flow immunoassay [170,171].

For long-term storage and use of nanodiagnostics, maintaining the stability of colloidal nanomaterials remains a challenge in the field. For example, GNPs are known to aggregate especially in the presence of certain biological molecules like nucleic acids and proteins, or high salts [175]. QD encoded microbeads tend to break down at high pH (>8) and temperature (>40 °C) [93]. Also, fouling can happen at the surface of colloidal nanomaterials due to non-specific adsorption of molecules, which can alter the original function of these materials. Hence, there needs to be a persistent effort towards making good quality particles, and developing strategies to store these particles for maintaining the quality and long-term usage.

Lastly, once the all-in-one device is implemented in the field, diagnostic efficacy can be evaluated by conducting a prospective study over a patient cohort. Diagnostic efficacy evaluates the product of the diagnostic accuracy and clinical effectiveness from the implementation of a new diagnostic test [176]. For instance, it can be defined as the product of positive likelihood ratio and patient notification rate, in which the positive likelihood ratio is calculated as the sensitivity divided by 1 minus specificity, and the patient notification rate is the percentage of patients receiving diagnostic results over a fixed time [176]. Alternatively, these terms can be replaced with other clinical metrics that are used to characterize diagnostic accuracy and clinical effectiveness such as the area under the curve (AUC) of a ROC plot, rate of antibiotic misuse, and time to treatment initiation. This metric can therefore be used to describe the overall diagnostic performance by capturing the aspect of patient outcome from the implementation of a new diagnostic test in the field, and accounting for test inaccuracies, delays and clinical consequences as a result of missing or delaying diagnosis [176].

While many of the diagnostic technologies are in the early development, there are a number of notable nanodiagnostics used in the clinic. LFA is a widely used diagnostic system for infectious pathogens. For instance, OraQuick (OraSure Technologies) is a LFA-based HIV test, which gained FDA approval in 2012, and is being sold over-the-counter in the United States. More recently, Mirkin's bio-barcode assay also demonstrated successful translation into the clinics. Bio-barcode assay technology formed the foundation of The Verigene System® (Luminex Corporation), which is FDA-cleared and used by healthcare professionals across different hospitals in the United States. Currently there are Verigene® Bloodstream, Gastrointestinal, and Respiratory Tract Infection tests available, which can be used to identify bacteria and antibiotic resistance from blood cultures, determine gastrointestinal infection from stool samples, and diagnose viral infections respectively. Most recently, Sia's mChip technology is demonstrating a potential success towards translation [177]. mChip technology utilizes a patented microfluidic system with GNP signal amplification to deliver a highly sensitive, quantitative and convenient immunodiagnostic test [178]. This technology was further developed in Claros Diagnostics, which was acquired by OPKO Health Inc. for $30 million

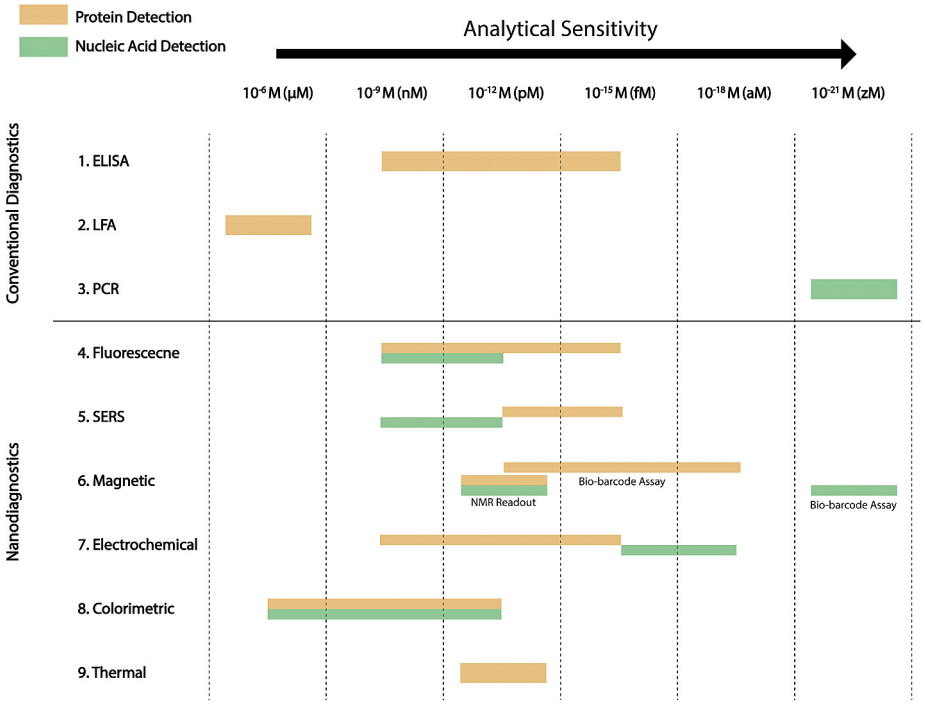

Fig. 11. Comparison of Analytical Sensitivities. Analytical sensitivities of nanodiagnostics in comparison to conventional diagnostic methods for detection of proteins and nucleic acids.

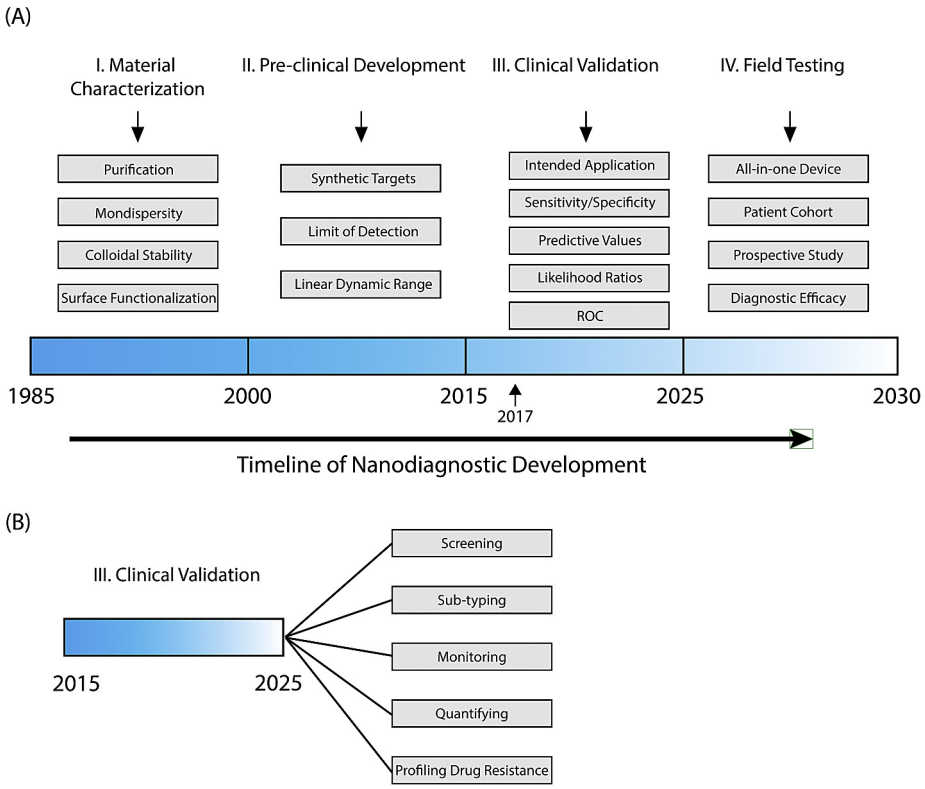

Fig. 12. Timeline of Nanodiagnostic Development. (A) Nanodiagnostic development is categorized into four stages: I. Material Characterization, II. Pre-clinical Development, III. Clinical Validation, and IV. Field Testing. (B) The intended diagnostic application (i.e. screening, sub-typing, monitoring, quantifying, or profiling drug resistance) can be determined upon the completion of clinical validation.

Table 2
Metrics for clinical validation of nanodiagnostics.[a]

Term	Equation	Description
True Positive	–	A positive test result given by the diagnostic assay under evaluation that matches that of the reference standard
True Negative	–	A negative test result given by the diagnostic assay under evaluation that matches that of the reference standard
False Positive	–	A positive test result given by the diagnostic assay under evaluation that does not match that of the reference standard
False Negative	–	A negative test result given by the diagnostic assay under evaluation that does not match that of the reference standard
Sensitivity	$\frac{True\ Positives}{True\ Positive+False\ Negatives}$	The predicted percent of true positives among all positive test results obtained by the reference standard
Specificity	$\frac{True\ Negatives}{True\ Negatives+False\ Positives}$	The predicted percent of true negatives among all negative test results obtained by the reference standard
Positive Predictive Value	$\frac{True\ Positives}{True\ Positive+False\ Positives}$	The predicted percent of true positive among all positive test results obtained by the diagnostic assay under evaluation
Negative Predictive Value	$\frac{True\ Negatives}{True\ Negatives+False\ Negatives}$	The predicted percent of true negatives among all negative test results obtained by the diagnostic assay under evaluation
Positive Likelihood Ratio	$\frac{Sensitivity}{1-Specificity}$	The odds of the test under evaluation to produce a positive test result when the disease is present *versus* a positive test result when the disease is absent
Negative Likelihood Ratio	$\frac{1-Sensitivity}{Specificity}$	The odds of the test under evaluation to produce a positive test result when the disease is absent *versus* a negative test result when the disease is absent
Diagnostic Odds Ratio	$\frac{True\ Positives/\ False\ Positives}{False\ Negatives/True\ Negatives}$	The ratio of the odds of the test under evaluation to produce a positive result if the subject has a disease relative to the odds of producing a positive result if the subject does not have the disease
Receiver Operator Characteristic Curve	–	The curve produced when true positives on the y-axis are compared against false positives on the x-axis, for a range of cutoff values for the diagnostic test under evaluation

[a] Table adapted from source [172].

dollars in 2011. Claros® 1 and Claros® 1 Total Prostate Specific Antigen (PSA) are currently pending FDA clearance.

6. Conclusion

The 20th century has witnessed a tremendous effort in the development and improvement of diagnostic tests to combat infectious diseases. Rapid and early diagnosis of infections will help to prevent the transmission of diseases, and enable healthcare workers to provide an appropriate treatment in a time-effective manner. This can improve treatment outcomes, reduce healthcare costs, and decrease the risk of developing antimicrobial resistance, especially in low-income countries.

As we discussed in this review article, nanoparticles have been exploited to improve the analytical sensitivity of diagnostic assays, provide various readout signals, simultaneously detect multiple targets, and simplify diagnostic procedures. For instance, GNPs were used to improve the analytical sensitivity of EC and SERS based assays for detection of pathogens at a single-cell sensitivity level. Additionally, nanoparticles can be designed for colorimetric, thermal, fluorescence, magnetic, electrochemical and Raman signal readouts. This provides versatility in designing diagnostic systems. Furthermore, the ability to easily fine-tune the fluorescence emission of QDs in the visible spectrum, and incorporation of them into polymeric microbeads have provided a versatile multiplex diagnostic platform that can detect a variety of disease biomarkers at the same time. Lastly, MNPs provided a simple method to extract biological targets from clinical specimens without using a centrifuge device, and facilitate washing steps in a molecular assay.

The benefits of nanodiagnostics demonstrate a great potential in many diagnostic applications, especially for use in POC testing; however, there are many barriers to transitioning their utility in the field. Foremost, current nanodiagnostics include steps that involve sample extraction, purification, and detection, which all involve extensive pipetting performed by skilled workers. This complexity, however, could be addressed by engineering a portable all-in-one device that automates the diagnostic procedure, and minimize labor work. Secondly, many nanodiagnostic assays are in the preclinical stage, and a clinical validation using large set of patient samples is required to fully assess the capability of these techniques in a real clinical context [172]. Clinical assessment of nanodiagnostic technologies early in the development process can accelerate their translation because there are many variables with patient samples that can be incorporated in the design process. Nanodiagnostic community therefore, should focus on addressing these challenges, which in effect will advance the implementation of nanodiagnostics for detection of infectious diseases in POC settings.

References

[1] M.L. Barreto, M.G. Teixeira, E.H. Carmo, Infectious diseases epidemiology, J. Epidemiol. Community Health 60 (2006) 192–195, http://dx.doi.org/10.1136/jech.2003.011593.
[2] M.E.J. Woolhouse, S. Gowtage-Sequeria, Host range and emerging and reemerging pathogens, Emerg. Infect. Dis. 11 (2005) 1842–1847, http://dx.doi.org/10.3201/eid1112.050997.
[3] L.H. Taylor, S.M. Latham, M.E.J. Woolhouse, S.M. Lathamt, E. Bush, Risk factors Hum. Dis. Emergence 356 (2013) 983–989, http://dx.doi.org/10.1098/rstb.2001.0888.
[4] S.I. Hay, K.E. Battle, D.M. Pigott, D.L. Smith, C.L. Moyes, S. Bhatt, et al., Global mapping of infectious disease, philosophical transactions of the royal society of london. Series B, Biol. Sci. 368 (2013), 20120250, http://dx.doi.org/10.1098/rstb.2012.0250.
[5] S. Cleaveland, M.K. Laurenson, L.H. Taylor, Diseases of humans and their domestic mammals: pathogen characteristics, host range and the risk of emergence, Philosophical Transactions of the Royal Society of London. Series B, Biol. Sci. 356 (2001) 991–999, http://dx.doi.org/10.1098/rstb.2001.0889.
[6] K.E. Jones, N.G. Patel, M.A. Levy, A. Storeygard, D. Balk, J.L. Gittleman, et al., Global trends in emerging infectious diseases, Nature 451 (2008) 990–993, http://dx.doi.org/10.1038/nature06536.
[7] A.S. Fauci, N.A. Touchette, G.K. Folkers, Emerging infectious diseases: a 10-year perspective from the national institute of allergy and infectious diseases, Emerg. Infect. Dis. 11 (2005) 519–525.
[8] World Health Organization, World Health Statistics 2009, 2009, p. 47.
[9] H.C. Neu, The crisis in antibiotic resistance, Sci. (New York, N.Y.) 257 (1992) 1064–1073, http://dx.doi.org/10.1126/science.257.5073.1064.
[10] J. O'Neill, Antimicrobial resistance: tackling a crisis for the health and wealth of nations, Rev. Antimicrob. Resist. 91 (2014) 1–16.
[11] J.W. Sanders, G.S. Fuhrer, M.D. Johnson, M.S. Riddle, The epidemiological transition: the current status of infectious diseases in the developed world versus the developing world, Sci. Prog. 91 (2008) 1–38, http://dx.doi.org/10.3184/003685008X284628.
[12] R.B. Turner, Epidemiology, pathogenesis, and treatment of the common cold, annals of allergy, Asthma Immunol. 78 (1997) 531–540, http://dx.doi.org/10.1016/S1081-1206(10)63213-9.
[13] I. Gupta, P. Guin, Communicable diseases in the south-east asia region of the world health organization: towards a more effective response, Bull. World Health Organ. 88 (2010) 199–205, http://dx.doi.org/10.2471/BLT.09.065540.
[14] N.S. Zhong, B.J. Zheng, Y.M. Li, L. Poon, Z.H. Xie, K.H. Chan, et al., Epidemiology and cause of severe acute respiratory syndrome (SARS) in Guangdong, People's Republic of China, in February, 2003, Lancet 362 (2003) 1353–1358, http://dx.doi.org/10.1016/S0140-6736(03)14630-2.
[15] G. Neumann, T. Noda, Y. Kawaoka, Emergence and pandemic potential of swine-origin H1N1 influenza virus, Nature 459 (2009) 931–939, http://dx.doi.org/10.1038/nature08157.
[16] L.O. Gostin, D. Lucey, A. Phelan, The Ebola epidemic, Jama 312 (2014)

1095–1096, http://dx.doi.org/10.1001/jama.2014.11176.
[17] U. Samarasekera, M. Triunfol, Concern over Zika virus grips the world, Lancet 387 (2016) 521–524, http://dx.doi.org/10.1016/S0140-6736(16)00257-9.
[18] L.P. Balogh, Why do we have so many definitions for nanoscience and nanotechnology? Nanomed. Nanotechnol. Biol. Med. 6 (2010) 397–398, http://dx.doi.org/10.1016/j.nano.2010.04.001.
[19] B.Y.S. Kim, J.T. Rutka, W.C.W. Chan, Nanomedicine, N. Engl. J. Med. 363 (2010) 2434–2443.
[20] S. Link, M.A. El-Sayed, Shape and size dependence of radiative, non-radiative and photothermal properties of gold nanocrystals, Int. Rev. Phys. Chem. 19 (2000) 409–453.
[21] N.P. Pai, C. Vadnais, C. Denkinger, N. Engel, M. Pai, Point-of-Care testing for infectious diseases: diversity, complexity, and barriers in low- and middle-income countries, PLoS Med. 9 (2012), http://dx.doi.org/10.1371/journal.pmed.1001306.
[22] R.W. Peeling, D. Mabey, Point-of-care tests for diagnosing infections in the developing world, Clin. Microbiol. Infect. 16 (2010) 1062–1069, http://dx.doi.org/10.1111/j.1469-0691.2010.03279.x.
[23] S. Sharma, J. Zapatero-Rodr, I. guez, P. Estrela, R. O'Kennedy, Point-of-Care diagnostics in low resource settings: present status and future role of microfluidics, Biosensors 5 (2015) 577–601, http://dx.doi.org/10.3390/bios5030577.
[24] T. Albrecht, J.W. Almond, M.J. Alfa, G.G. Alton, R. Aly, D.M. Asher, et al., Medical Microbiology, 4 ed., 1996.
[25] C.K. Murray, R.A. Gasser, A.J. Magill, R.S. Miller, Update on rapid diagnostic testing for malaria, Clin. Microbiol. Rev. 21 (2008) 97–110, http://dx.doi.org/10.1128/CMR.00035-07.
[26] C. Wongsrichanalai, M.J. Barcus, S. Muth, A. Sutamihardja, W.H. Wernsdorfer, A review of malaria diagnostic tools: microscopy and rapid diagnostic test (RDT), Am. J. Trop. Med. Hyg. 77 (2007) 119–127.
[27] D. Payne, Use and limitations of light microscopy for diagnosing malar-iaattheprimaryhealthcarelevel, Bull. World Health Organ. 66 (1988) 621–626.
[28] K.R. Steingart, M. Henry, V. Ng, P.C. Hopewell, A. Ramsay, J. Cunningham, et al., Fluorescence versus conventional sputum smear microscopy for tuberculosis: a systematic review, Lancet Infect. Dis. 6 (2006) 570–581, http://dx.doi.org/10.1016/S1473-3099(06)70578-3.
[29] R. Singhal, V.P. Myneedu, Microscopy as a diagnostic tool in pulmonary tuberculosis, Int. J. Mycobacteriol. 4 (2015) 1–6, http://dx.doi.org/10.1016/j.ijmyco.2014.12.006.
[30] D. Vickers, T. Ahmad, M.G. Coulthard, Diagnosis of urinary tract infection in children: fresh urine microscopy or culture? Lancet 338 (1991) 767–770.
[31] M.L. Wilson, L. Gaido, Laboratory diagnosis of urinary tract infections in adult patients, Med. Microbiol. 38 (2004) 1150–1158.
[32] R.D. Jenkins, J.P. Fenn, J.M. Matsen, Review of urine microscopy for bacteriuria, Jama 255 (1986) 3397–3403.
[33] F.B. Tek, A.G. Dempster, I. Kale, Computer vision for microscopy diagnosis of malaria, Malar. J. 8 (2009) 153–167, http://dx.doi.org/10.1186/1475-2875-8-153.
[34] M.R. Pulido, M. Garcia-Quintanilla, R. Martin-Pena, J.M. Cisneros, M.J. McConnell, Progress on the development of rapid methods for antimicrobial susceptibility testing, J. Antimicrob. Chemother. 68 (2013) 2710–2717, http://dx.doi.org/10.1093/jac/dkt253.
[35] J.H. Jorgensen, M.J. Ferraro, Antimicrobial susceptibility testing: a review of general principles and contemporary practices, Clin. Infect. Dis. 49 (2009) 1749–1755, http://dx.doi.org/10.1086/647952.
[36] J.H. Jorgensen, M.J. Ferraro, Antimicrobial susceptibility testing: a review of general principles and contemporary practices, Clin. Infect. Dis. 49 (2009) 1749–1755, http://dx.doi.org/10.1086/647952.
[37] J.M. Andrews, J.M. Andrews, Determination of minimum inhibitory concentrations, J. Antimicrob. Chemother. 48 (Suppl 1) (2001) 5–16, http://dx.doi.org/10.1093/jac/48.suppl_1.5.
[38] CLSI, Performance Standards for Antimicrobial Susceptibility Testing; Twenty-fifth Informational Supplement, CLSI Document M100-S25. 35, 2015.
[39] D.H. Bergey, Bacteroidetes, Bergey's Manual of Systematic Bacteriology, vol. 4, 2010, http://dx.doi.org/10.1007/978-0-387-68572-4.
[40] S.D. Gan, K.R. Patel, Enzyme immunoassay and enzyme-linked immunosorbent assay, J. Invest. Dermatol. 133 (2013) e12–e14, http://dx.doi.org/10.1038/jid.2013.287.
[41] P.F. Wright, E. Nilsson, E.M.A. Vanrooij, M. Lelenta, M.H. Jeggo, Standardisation and validation of enzyme-linked immunosorbent assay techniques for the detection of antibody in infectious disease diagnosis, Rev. Sci. Tech. Off. Int. Epiz 12 (1993) 435–450.
[42] C. Torres, V. Linder, B.A. Parviz, A. Siegel, G.M. Whitesides, An integrated approach to a portable and low-cost immunoassay for resource-poor settings 43 (2004) 498–502, http://dx.doi.org/10.1002/anie.200353016.
[43] X.J. Li, Z.H. Nie, C.M. Cheng, A.B. Goodale, G.M. Whitesides, Paper-based electrochemical elisa, in: 14th International Conference on Miniaturized Systems for Chemistry and Life Sciences, 2010, pp. 1487–1489.
[44] G.A. Posthuma-Trumpie, J. Korf, A. van Amerongen, Lateral flow (immuno) assay: its strengths, weaknesses, opportunities and threats. A literature survey, Anal. Bioanal. Chem. 393 (2009) 569–582, http://dx.doi.org/10.1007/s00216-008-2287-2.
[45] B.A. Rohrman, V. Leautaud, E. Molyneux, R.R. Richards-Kortum, A lateral flow assay for quantitative detection of amplified HIV-1 RNA, PLoS One 7 (2012), http://dx.doi.org/10.1371/journal.pone.0045611.
[46] N. Tangpukdee, C. Duangdee, P. Wilairatana, S. Krudsood, Malaria diagnosis: a brief review, Korean J. Parasitol. 47 (2009) 93–102, http://dx.doi.org/10.3347/kjp.2009.47.2.93.
[47] J.E. Vidal, D.R. Boulware, Lateral flow assay for cryptococcal antigen: an important advance to improve the continuum of hiv care and reduce cryptococcal meningitis-related mortality, Rev. Inst. Med. Trop. Sao Paulo 57 (2015) 38–45, http://dx.doi.org/10.1590/S0036-46652015000700008.
[48] G.A. Posthuma-Trumpie, J. Korf, A. van Amerongen, Lateral flow (immuno) assay: its strengths, weaknesses, opportunities and threats. A literature survey, Anal. Bioanal. Chem. 393 (2008) 569–582, http://dx.doi.org/10.1007/s00216-008-2287-2.
[49] C.A. Heid, J. Stevens, K.J. Livak, P.M. Williams, Real time quantitative PCR, Genome Res. 6 (1996) 986–994.
[50] B. Vogelstein, K.W. Kinzler, Digital PCR, Proc. Natl. Acad. Sci. U. S. A. 96 (1999) 9236–9241.
[51] J.A. Sanchez, K.E. Pierce, J.E. Rice, L.J. Wangh, Linear-After-The-Exponential (LATE)–PCR: an advanced method of asymmetric PCR and its uses in quantitative real-time analysis, Proc. Natl. Acad. Sci. U. S. A. 101 (2004) 1933–1938.
[52] S.A. Bustin, Quantification of mRNA using real-time reverse transcription PCR (RT-PCR): trends and problems, J. Mol. Endocrinol. 29 (2002) 23–39.
[53] O. Henegariu, N.A. Heerema, S.R. Dlouhy, G.H. Vance, P.H. Vogt, Multiplex PCR: critical parameters and step-by-step protocol, BioTechniques. 23 (1997) 504–511.
[54] M.C. Edwards, R.A. Gibbs, Multiplex PCR: advantages, development and applications, Genome Res. 3 (1994) S65–S75.
[55] K. Mullis, F. Faloona, S. Scharf, R. Saiki, G. Horn, H. Erlich, Specific Enzymatic Amplification of DNA in Vitro: the Polymerase Chain Reaction, Cold Spring Harbor Symposia on Quantitative Biology, 1986, pp. 263–273.
[56] J.-M. Nam, S.I. Stoeva, C.A. Mirkin, Bio-Bar-Code-based DNA detection with PCR-like sensitivity, J. Am. Chem. Soc. 126 (2004) 5932–5933, http://dx.doi.org/10.1021/ja049384.
[57] M.J. Espy, J.R. Uhl, L.M. Sloan, S.P. Buckwalter, M.F. Jones, E.A. Vetter, et al., Real-time PCR in clinical Microbiology: applications for routine laboratory testing, Clin. Microbiol. Rev. 19 (2006) 165–256, http://dx.doi.org/10.1128/CMR.19.1.165-256.2006.
[58] S. Park, Y. Zhang, S. Lin, T.-H. Wang, S. Yang, Advances in microfluidic PCR for point-of-care infectious disease diagnostics, Biotechnol. Adv. 29 (2011) 830–839, http://dx.doi.org/10.1016/j.biotechadv.2011.06.017.
[59] V. Ravi, V. Potdar, S.N. Madhusudana, R. Bhatia, A. Desai, L. Aung, et al., Establishment of PCR Laboratory in Developing Countries, 2011.
[60] A. Niemz, T.M. Ferguson, D.S. Boyle, Point-of-care nucleic acid testing for infectious diseases, Trends Biotechnol. 29 (2011) 240–250, http://dx.doi.org/10.1016/j.tibtech.2011.01.007.
[61] R. Sanjuan, M.R. Nebot, N. Chirico, L.M. Mansky, R. Belshaw, Viral mutation rates, J. Virol. 84 (2010) 9733–9748, http://dx.doi.org/10.1128/JVI.00694-10.
[62] P. Reiss, M. Protière, L. Li, Core/shell semiconductor nanocrystals, Small 5 (2009) 154–168, http://dx.doi.org/10.1002/smll.200800841.
[63] A.P. Alivisatos, Semiconductor clusters, nanocrystals, and quantum dots, Science 271 (1996) 933–937.
[64] B.A. Kairdolf, A.M. Smith, T.H. Stokes, M.D. Wang, A.N. Young, S. Nie, Semiconductor quantum dots for bioimaging and biodiagnostic applications, Annu. Rev. Anal. Chem. 6 (2013) 143–162, http://dx.doi.org/10.1146/annurev-anchem-060908-155136.
[65] P. Alivisatos, The use of nanocrystals in biological detection, Nat. Biotechnol. 22 (2003) 47–52, http://dx.doi.org/10.1038/nbt927.
[66] Z. Jin, N. Hildebrandt, Semiconductor quantum dots for in vitro diagnostics and cellular imaging, Trends Biotechnol. 30 (2012) 394–403, http://dx.doi.org/10.1016/j.tibtech.2012.04.005.
[67] W.C.W. Chan, S. Nie, Quantum dot bioconjugates for ultrasensitive nonisotopic detection, Science 281 (1998) 2016–2018.
[68] N.R. Isola, D.L. Stokes, T. Vo-Dinh, Surface-enhanced raman gene probe for HIV detection, Anal. Chem. 70 (1998) 1352–1356.
[69] D. Schaming, H. Remita, Nanotechnology: from the ancient time to nowadays, Found. Chem. 17 (2015) 187–205, http://dx.doi.org/10.1007/s10698-015-9235-y.
[70] K.L. Kelly, E. Coronado, L.L. Zhao, G.C. Schatz, The optical properties of metal nanoparticles: the influence of size, shape, and dielectric environment, J. Phys. Chem. B 107 (2003) 668–677, http://dx.doi.org/10.1021/jp026731y.
[71] S.K. Ghosh, T. Pal, Interparticle coupling effect on the surface plasmon resonance of gold nanoparticles: from theory to applications, Chem. Rev. 107 (2007) 4797–4862, http://dx.doi.org/10.1021/cr0680282.
[72] J. Gao, C.M. Bender, C.J. Murphy, Dependence of the gold nanorod aspect ratio on the nature of the directing surfactant in aqueous solution, Langmuir 19 (2003) 9065–9070, http://dx.doi.org/10.1021/la034919i.
[73] R. Elghanian, J.J. Storhoff, R.C. Mucic, R.L. Letsinger, C.A. Mirkin, Selective colorimetric detection of polynucleotides based on the distance-dependent optical properties of gold nanoparticles, Science 277 (1997) 1078–1081.
[74] P.K. Jain, X. Huang, I.H. El-Sayed, M.A. El-Sayed, Noble metals on the nanoscale: optical and photothermal properties and some applications in imaging, sensing, biology, and medicine, Accounts Chem. Res. 41 (2008) 1578–1586, http://dx.doi.org/10.1021/ar7002804.
[75] L.H. Reddy, J.L. Arias, J. Nicolas, P. Couvreur, Magnetic nanoparticles: design and characterization, toxicity and biocompatibility, pharmaceutical and

biomedical applications, Chem. Rev. 112 (2012) 5818–5878, http://dx.doi.org/10.1021/cr300068p.
[76] S. Prijic, G. Sersa, Magnetic nanoparticles as targeted delivery systems in oncology, Radiol. Oncol. 45 (2011) 1–16, http://dx.doi.org/10.2478/v10019-011-0001-z.
[77] Z. Zou, D. Du, J. Wang, J.N. Smith, C. Timchalk, Y. Li, et al., Quantum dot-based immunochromatographic fluorescent biosensor for biomonitoring trichloropyridinol, a biomarker of exposure to chlorpyrifos, Anal. Chem. 82 (2010) 5125–5133, http://dx.doi.org/10.1021/ac100260m.
[78] X. Xu, X. Liu, Z. Nie, Y. Pan, M. Guo, S. Yao, Label-Free fluorescent detection of protein kinase activity based on the aggregation behavior of unmodified quantum dots, Anal. Chem. 83 (2011) 52–59, http://dx.doi.org/10.1021/ac102786c.
[79] C. Peng, Z. Li, Y. Zhu, W. Chen, Y. Yuan, L. Liu, et al., Simultaneous and sensitive determination of multiplex chemical residues based on multicolor quantum dot probes, Biosens. Bioelectron. 24 (2009) 3657–3662, http://dx.doi.org/10.1016/j.bios.2009.05.031.
[80] J. Park, Y. Park, S. Kim, Signal amplification via biological self-assembly of surface-engineered quantum dots for multiplexed subattomolar immunoassays and apoptosis imaging, ACS Nano 7 (2013) 9416–9427, http://dx.doi.org/10.1021/nn4042078.
[81] C.-Y. Zhang, J. Hu, Single quantum dot-based nanosensor for multiple DNA detection, Anal. Chem. 82 (2010) 1921–1927, http://dx.doi.org/10.1021/ac9026675.
[82] I.L. Medintz, A.R. Clapp, H. Mattoussi, E.R. Goldman, B. Fisher, J.M. Mauro, Self-assembled nanoscale biosensors based on quantum dot FRET donors, Nat. Mater. 2 (2003) 630–638, http://dx.doi.org/10.1038/nmat961.
[83] C.-Y. Zhang, L.W. Johnson, Quantum-Dot-based nanosensor for RRE IIB RNA–Rev peptide interaction assay, J. Am. Chem. Soc. 128 (2006) 5324–5325, http://dx.doi.org/10.1021/ja060537y.
[84] M. Han, X. Gao, J.Z. Su, S. Nie, Quantum-dot-tagged microbeads for multiplexed optical coding of biomolecules, Nat. Biotechnol. 19 (2001) 631–635.
[85] J.M. Klostranec, Q. Xiang, G.A. Farcas, J.A. Lee, A. Rhee, E.I. Lafferty, et al., Convergence of quantum dot barcodes with microfluidics and signal processing for multiplexed high-throughput infectious disease diagnostics, Nano Lett. 7 (2007) 2812–2818, http://dx.doi.org/10.1021/nl071415m.
[86] S. Giri, E.A. Sykes, T.L. Jennings, W.C.W. Chan, Rapid screening of genetic biomarkers of infectious agents using quantum dot barcodes, ACS Nano 5 (2011) 1580–1587, http://dx.doi.org/10.1021/nn102873w.
[87] E. Sharon, R. Freeman, I. Willner, CdSe/zns quantum dots-g-Quadruplex/hemin hybrids as optical DNA sensors and aptasensors, Anal. Chem. 82 (2010) 7073–7077, http://dx.doi.org/10.1021/ac101456x.
[88] G. Jiang, A.S. Susha, A.A. Lutich, F.D. Stefani, J. Feldmann, A.L. Rogach, Cascaded FRET in conjugated polymer/quantum dot/dye-labeled DNA complexes for DNA hybridization detection, ACS Nano 3 (2009) 4127–4131, http://dx.doi.org/10.1021/nn901324y.
[89] R. Freeman, Y. Li, R. Tel-Vered, E. Sharon, J. Elbaz, I. Willner, Self-assembly of supramolecular aptamer structures for optical or electrochemical sensing, Analyst 134 (2009) 653–654, http://dx.doi.org/10.1039/b822836c.
[90] C.-W. Chi, Y.-H. Lao, Y.-S. Li, L.-C. Chen, A quantum dot-aptamer beacon using a DNA intercalating dye as the FRET reporter: application to label-free thrombin detection, Biosens. Bioelectron. 26 (2011) 3346–3352, http://dx.doi.org/10.1016/j.bios.2011.01.015.
[91] S. Fournier Bidoz, T.L. Jennings, J.M. Klostranec, W. Fung, A. Rhee, D. Li, et al., Facile and rapid one-step mass preparation of quantum-dot barcodes, Angew. Chem. 47 (2008) 5577–5581, http://dx.doi.org/10.1002/anie.200800409.
[92] G. Wang, Y. Leng, H. Dou, L. Wang, W. Li, X. Wang, et al., Highly efficient preparation of multiscaled quantum dot barcodes for multiplexed hepatitis B detection, ACS Nano 7 (2013) 471–481, http://dx.doi.org/10.1021/nn3045215.
[93] K. Chen, L.Y.T. Chou, F. Song, W.C.W. Chan, Fabrication of metal nanoshell quantum-dot barcodes for biomolecular detection, Nano Today 8 (2013) 228–234, http://dx.doi.org/10.1016/j.nantod.2013.04.009.
[94] J. Kim, M.J. Biondi, J.J. Feld, W.C.W. Chan, Clinical validation of quantum dot barcode diagnostic technology, ACS Nano 10 (2016) 4742–4753, http://dx.doi.org/10.1021/acsnano.6b01254.
[95] E. Dulkeith, A.C. Morteani, T. Niedereichholz, T.A. Klar, J. Feldmann, S.A. Levi, et al., Fluorescence quenching of dye molecules near gold nanoparticles: radiative and nonradiative effects, Phys. Rev. Lett. 89 (2002), 203002, http://dx.doi.org/10.1103/PhysRevLett.89.203002.
[96] D.J. Maxwell, J.R. Taylor, S. Nie, Self-Assembled nanoparticle probes for recognition and detection of biomolecules, J. Am. Chem. Soc. 124 (2002) 9606–9612, http://dx.doi.org/10.1021/ja025814p.
[97] A. Samanta, Y. Zhou, S. Zou, H. Yan, Y. Liu, Fluorescence quenching of quantum dots by gold nanoparticles: a potential long range spectroscopic ruler, Nano Lett. 14 (2014) 5052–5057, http://dx.doi.org/10.1021/nl501709s.
[98] B. Nikoobakht, C. Burda, M. Braun, M. Hun, M.A. El-Sayed, The quenching of CdSe quantum dots photoluminescence by gold nanoparticles in solution, Photochem. Photobiol. 75 (2002) 591–597, http://dx.doi.org/10.1562/0031-8655(2002)0750591TQOCQD2.0.CO2.
[99] N.N. Horimoto, K. Imura, H. Okamoto, Chem. Phys. Lett. (2008), http://dx.doi.org/10.1016/j.cplett.2008.10.067.
[100] C. Xue, Y. Xue, L. Dai, A. Urbas, Q. Li, Size- and shape-dependent fluorescence quenching of gold nanoparticles on perylene dye, Adv. Opt. Mater. 1 (2013) 581–587, http://dx.doi.org/10.1002/adom.201300175.
[101] S. Mayilo, M.A. Kloster, M. Wunderlich, A. Lutich, T.A. Klar, A. Nichtl, et al., Long-range fluorescence quenching by gold nanoparticles in a sandwich immunoassay for cardiac troponin T, Nano Lett. 9 (2009) 4558–4563, http://dx.doi.org/10.1021/nl903178n.
[102] B. Dubertret, M. Calame, A.J. Libchaber, Single-mismatch detection using gold-quenched fluorescent oligonucleotides, Nat. Biotechnol. 19 (2001) 365–370, http://dx.doi.org/10.1038/86762.
[103] S. Song, Z. Liang, J. Zhang, L. Wang, G. Li, C. Fan, Gold-nanoparticle-based multicolor nanobeacons for sequence-specific DNA analysis, Angew. Chem. Int. Ed. 48 (2009) 8670–8674, http://dx.doi.org/10.1002/anie.200901887.
[104] H.-Y. Yeh, M.V. Yates, A. Mulchandani, W. Chen, Molecular beacon–quantum dot–Au nanoparticle hybrid nanoprobes for visualizing virus replication in living cells, Chem. Commun. 46 (2010) 3914–3916, http://dx.doi.org/10.1039/c001553a.
[105] L. Chen, S. Neethirajan, A homogenous fluorescence quenching based assay for specific and sensitive detection of influenza virus a hemagglutinin antigen, Sensors 15 (2015) 8852–8865, http://dx.doi.org/10.3390/s150408852.
[106] S. He, B. Song, D. Li, C. Zhu, W. Qi, Y. Wen, et al., A graphene nanoprobe for rapid, sensitive, and multicolor fluorescent DNA analysis, Adv. Funct. Mater 20 (2010) 453–459, http://dx.doi.org/10.1002/adfm.200901639.
[107] F. Li, Y. Huang, Q. Yang, Z. Zhong, D. Li, L. Wang, et al., A graphene-enhanced molecular beacon for homogeneous DNA detection, Nanoscale 2 (2010) 1021–1026, http://dx.doi.org/10.1039/b9nr00401g.
[108] H. Dong, W. Gao, F. Yan, H. Ji, H. Ju, Fluorescence resonance energy transfer between quantum dots and graphene oxide for sensing biomolecules, Anal. Chem. 82 (2010) 5511–5517, http://dx.doi.org/10.1021/ac100852z.
[109] C.-H. Lu, H.-H. Yang, C.-L. Zhu, X. Chen, G.-N. Chen, A graphene platform for sensing biomolecules, Angew. Chem. Int. Ed. 48 (2009) 4785–4787, http://dx.doi.org/10.1002/anie.200901479.
[110] J. Ni, R.J. Lipert, G.B. Dawson, M.D. Porter, Immunoassay readout method using extrinsic raman labels adsorbed on immunogold colloids, Anal. Chem. 71 (1999) 4903–4908, http://dx.doi.org/10.1021/ac990616a.
[111] L. Sun, C. Yu, J. Irudayaraj, Raman multiplexers for alternative gene splicing, Anal. Chem. 80 (2008) 3342–3349, http://dx.doi.org/10.1021/ac702542n.
[112] B.-H. Jun, J.-H. Kim, H. Park, J.S. Kim, K.N. Yu, S.-M. Lee, et al., Surface-enhanced raman spectroscopic-encoded beads for multiplex immunoassay, J. Comb. Chem. 9 (2007) 237–244, http://dx.doi.org/10.1021/cc0600831.
[113] Y.S. Huh, A.J. Chung, D. Erickson, Surface enhanced Raman spectroscopy and its application to molecular and cellular analysis, Microfluid Nanofluid 6 (2009) 285–297, http://dx.doi.org/10.1007/s10404-008-0392-3.
[114] P.G. Etchegoin, E.C. Le Ru, A perspective on single molecule SERS: current status and future challenges, Phys. Chem. Chem. Phys. 10 (2008) 6079–6089, http://dx.doi.org/10.1039/b809196j.
[115] K. Kneipp, H. Kneipp, V.B. Kartha, R. Manoharan, G. Deinum, I. Itzkan, et al., Detection and identification of a single DNA base molecule using surface-enhanced Raman scattering (SERS), Phys. Rev. E 57 (1998) R6281–R6284, http://dx.doi.org/10.1103/PhysRevE.57.R6281.
[116] Y.S. Huh, A.J. Chung, B. Cordovez, D. Erickson, Enhanced on-chip SERS based biomolecular detection using electrokinetically active microwells, Lab a Chip 9 (2009) 433–439, http://dx.doi.org/10.1039/B809702J.
[117] M.B. Wabuyele, T. Vo-Dinh, Detection of human immunodeficiency virus type 1 DNA sequence using plasmonics nanoprobes, Anal. Chem. 77 (2005) 7810–7815, http://dx.doi.org/10.1021/ac0514671.
[118] S. Xu, X. Ji, W. Xu, X. Li, L. Wang, Y. Bai, et al., Immunoassay using probe-labelling immunogold nanoparticles with silver staining enhancement via surface-enhanced Raman scattering, Analyst 129 (2004) 63–66, http://dx.doi.org/10.1039/b313094k.
[119] K. Kong, C. Kendall, N. Stone, I. Notingher, Raman spectroscopy for medical diagnostics — from in-vitro biofluid assays to in-vivo cancer detection, Adv. Drug Deliv. Rev. 89 (2015) 121–134, http://dx.doi.org/10.1016/j.addr.2015.03.009.
[120] H. Zhou, D. Yang, N.P. Ivleva, N.E. Mircescu, R. Niessner, C. Haisch, SERS detection of bacteria in water by in situ coating with Ag nanoparticles, Anal. Chem. 86 (2014) 1525–1533, http://dx.doi.org/10.1021/ac402935p.
[121] K. Gracie, E. Correa, S. Mabbott, J.A. Dougan, D. Graham, R. Goodacre, et al., Simultaneous detection and quantification of three bacterial meningitis pathogens by SERS, Chem. Sci. 5 (2014) 1030–1040, http://dx.doi.org/10.1039/C3SC52875H.
[122] S. Shanmukh, L. Jones, J. Driskell, Y. Zhao, R. Dluhy, R.A. Tripp, Rapid and sensitive detection of respiratory virus molecular signatures using a silver nanorod array SERS substrate, Nano Lett. 6 (2006) 2630–2636, http://dx.doi.org/10.1021/nl061666f.
[123] J. Neng, M.H. Harpster, W.C. Wilson, P.A. Johnson, Surface-enhanced Raman scattering (SERS) detection of multiple viral antigens using magnetic capture of SERS-active nanoparticles, Biosens. Bioelectron. 41 (2013) 316–321, http://dx.doi.org/10.1016/j.bios.2012.08.048.
[124] G. Breuzard, J.F. Angiboust, P. Jeannesson, M. Manfait, J.M. Millot, Surface-enhanced Raman scattering reveals adsorption of mitoxantrone on plasma membrane of living cells, Biochem. Biophys. Res. Commun. 320 (2004) 615–621, http://dx.doi.org/10.1016/j.bbrc.2004.05.203.
[125] Y. Gao, A.W.Y. Lam, W.C.W. Chan, Automating quantum dot barcode assays using microfluidics and magnetism for the development of a point-of-care device, ACS Appl. Mater. Interfaces 5 (2013) 2853–2860, http://dx.doi.org/10.1021/am302633h.

[126] J.M. Nam, S.I. Stoeva, C.A. Mirkin, Bio-bar-code-based DNA detection with PCR-like sensitivity, J. Am. Chem. Soc. 126 (2004) 5932–5933, http://dx.doi.org/10.1021/ja049384+&iName=master.img-000.jpg&w=228&h=316.
[127] J.-M. Nam, C.S. Thaxton, C.A. Mirkin, Nanoparticle-based bio–bar codes for the ultrasensitive detection of proteins, Science 301 (2003) 1884–1886.
[128] H.J. Chung, C.M. Castro, H. Im, H. Lee, R. Weissleder, A magneto-DNA nanoparticle system for rapid detection and phenotyping of bacteria, Nat. Nanotechnol. 8 (2013) 369–375, http://dx.doi.org/10.1038/nnano.2013.70.
[129] M. Liong, A.N. Hoang, J. Chung, N. Gural, C.B. Ford, C. Min, et al., Magnetic barcode assay for genetic detection of pathogens, Nat. Commun. 4 (1AD) (2013) 1752–1759, http://dx.doi.org/10.1038/ncomms2745.
[130] J.B. Haun, C.M. Castro, R. Wang, V.M. Peterson, B.S. Marinelli, H. Lee, et al., Micro-nmr for rapid molecular analysis of human tumor Samples, Science 3 (2011) 1–13.
[131] H. Lee, E. Sun, D. Ham, R. Weissleder, Chip–NMR biosensor for detection and molecular analysis of cells, Nat. Med. 14 (2008) 869–874, http://dx.doi.org/10.1038/nm.1711.
[132] I. Koh, R. Hong, R. Weissleder, L. Josephson, Sensitive NMR sensors detect antibodies to influenza, Angew. Chem. Int. Ed. 47 (2008) 4119–4121, http://dx.doi.org/10.1002/anie.200800069.
[133] J.M. Perez, L. Josephson, T. O'Loughlin, D. Högemann, R. Weissleder, Magnetic relaxation switches capable of sensing molecular interactions, Nat. Biotechnol. 20 (2002) 816–820, http://dx.doi.org/10.1038/nbt720.
[134] J. Grimm, J.M. Perez, L. Josephson, R. Weissleder, Novel nanosensors for rapid analysis of telomerase activity, Cancer Res. 64 (2004) 639–643, http://dx.doi.org/10.1158/0008-5472.CAN-03-2798.
[135] H. Lee, T.-J. Yoon, J.-L. Figueiredo, F.K. Swirski, R. Weissleder, Rapid detection and profiling of cancer cells in fine-needle aspirates, Proc. Natl. Acad. Sci. U. S. A. 106 (2009) 12459–12464, http://dx.doi.org/10.1073/pnas.0902365106.
[136] N.J. Ronkainen, H.B. Halsall, W.R. Heineman, Electrochemical biosensors, Chem. Soc. Rev. 39 (2010) 1747–1763, http://dx.doi.org/10.1039/b714449k.
[137] C.G. Bauer, A.V. Eremenko, E. Ehrentreich-Forster, F.F. Bier, A. Makower, H.B. Halsall, et al., Zeptomole-detecting biosensor for alkaline phosphatase in an electrochemical immunoassay for 2,4-dichlorophenoxyacetic acid, Anal. Chem. 68 (1996) 2453–2458, http://dx.doi.org/10.1021/ac960218x.
[138] N.L. Rosi, C.A. Mirkin, Nanostructures in biodiagnostics, Chem. Rev. 105 (2005) 1547–1562, http://dx.doi.org/10.1021/cr030067f.
[139] J. Wang, A.-N. Kawde, M. Musameh, Carbon-nanotube-modified glassy carbon electrodes for amplified label-free electrochemical detection of DNA hybridization, Analyst 128 (2003) 912–915, http://dx.doi.org/10.1039/b303282e.
[140] R. Gasparac, B.J. Taft, M.A. Lapierre-Devlin, A.D. Lazareck, J.M. Xu, S.O. Kelley, J. Am. Chem. Soc. 126 (2004) 12270, http://dx.doi.org/10.1021/ja0458221.
[141] J. Li, H.T. Ng, A. Cassell, W. Fan, H. Chen, Q. Ye, et al., Carbon nanotube nanoelectrode array for ultrasensitive DNA detection, Nano Lett. 3 (2003) 597–602, http://dx.doi.org/10.1021/nl0340677.
[142] S. Aydinlik, D. Ozkan-Ariksoysal, P. Kara, A.A. Sayiner, M. Ozsoz, A nucleic acid-based electrochemical biosensor for the detection of influenza B virus from PCR samples using gold nanoparticle-adsorbed disposable graphite electrode and Meldola's blue as an intercalator, Anal. Methods 3 (2011) 1607–1608, http://dx.doi.org/10.1039/c1ay05146f.
[143] R.J. Chen, S. Bangsaruntip, K.A. Drouvalakis, N.W.S. Kam, M. Shim, Y. Li, et al., Noncovalent functionalization of carbon nanotubes for highly specific electronic biosensors, Proc. Natl. Acad. Sci. U. S. A. 100 (2003) 4984–4989, http://dx.doi.org/10.1073/pnas.0837064100.
[144] F. Patolsky, G. Zheng, O. Hayden, M. Lakadamyali, X. Zhuang, C.M. Lieber, Electrical detection of single viruses, Proc. Natl. Acad. Sci. U. S. A. 101 (2004) 14017–14022, http://dx.doi.org/10.1073/pnas.0406159101.
[145] Y. Wang, Z. Ye, Y. Ying, New trends in impedimetric biosensors for the detection of foodborne pathogenic bacteria, Sensors 12 (2012) 3449–3471, http://dx.doi.org/10.3390/s120303449.
[146] S.-J. Park, T.A. Taton, C.A. Mirkin, Array-based electrical detection of DNA with nanoparticle probes, Science 295 (2002) 1503–1506, http://dx.doi.org/10.1126/science.1067003.
[147] J. Wang, D. Xu, R. Polsky, Magnetically-induced solid-state electrochemical detection of DNA hybridization, J. Am. Chem. Soc. 124 (2002) 4208–4209, http://dx.doi.org/10.1021/ja0255709.
[148] K. Idegami, M. Chikae, K. Kerman, N. Nagatani, T. Yuhi, T. Endo, et al., Gold nanoparticle-based redox signal enhancement for sensitive detection of human chorionic gonadotropin hormone, Electroanalysis 20 (2008) 14–21, http://dx.doi.org/10.1002/elan.200704011.
[149] G. Liu, T.M.H. Lee, J. Wang, Nanocrystal-based bioelectronic coding of single nucleotide polymorphisms, J. Am. Chem. Soc. 127 (2005) 38–39, http://dx.doi.org/10.1021/ja043780a.
[150] N. Pires, T. Dong, U. Hanke, N. Hoivik, Recent developments in optical detection technologies in lab-on-a-chip devices for biosensing applications, Sensors 14 (2014) 15458–15479, http://dx.doi.org/10.3390/s140815458.
[151] C.A. Mirkin, R.L. Letsinger, R.C. Mucic, J.J. Storhoff, A DNA-based method for rationally assembling nanoparticles into macroscopic materials, Nature 382 (1996) 607–609.
[152] R.A. Reynolds, C.A. Mirkin, R.L. Letsinger, Homogeneous, nanoparticle-based quantitative colorimetric detection of oligonucleotides, J. Am. Chem. Soc. 122 (2000) 3795–3796, http://dx.doi.org/10.1021/ja000133k.
[153] M.S. Verma, J.L. Rogowski, L. Jones, F.X. Gu, Colorimetric biosensing of pathogens using gold nanoparticles, Biotechnol. Adv. 33 (2015) 666–680, http://dx.doi.org/10.1016/j.biotechadv.2015.03.003.
[154] W.-S. Chan, B.S.F. Tang, M.V. Boost, C. Chow, P.H.M. Leung, Detection of methicillin-resistant Staphylococcus aureus using a gold nanoparticle-based colourimetric polymerase chain reaction assay, Biosens. Bioelectron. 53 (2014) 105–111, http://dx.doi.org/10.1016/j.bios.2013.09.027.
[155] H. Deng, X. Zhang, A. Kumar, G. Zou, X. Zhang, X.-J. Liang, Long genomic DNA amplicons adsorption onto unmodified gold nanoparticles for colorimetric detection of Bacillus anthracis, Chem. Commun. (2012) 51–53, http://dx.doi.org/10.1039/c2cc37037a.
[156] C. Jung, J.W. Chung, U.O. Kim, M.H. Kim, H.G. Park, Real-time colorimetric detection of target DNA using isothermal target and signaling probe amplification and gold nanoparticle cross-linking assay, Biosens. Bioelectron. 26 (2011) 1953–1958, http://dx.doi.org/10.1016/j.bios.2010.07.088.
[157] C.S. Thaxton, D.G. Georganopoulou, C.A. Mirkin, Gold nanoparticle probes for the detection of nucleic acid targets, Clin. Chim. Acta 363 (2006) 120–126, http://dx.doi.org/10.1016/j.cccn.2005.05.042.
[158] A. Ogawa, M. Maeda, Simple and rapid colorimetric detection of cofactors of aptazymes using noncrosslinking gold nanoparticle aggregation, Bioorg. Med. Chem. Lett. 18 (2008) 6517–6520, http://dx.doi.org/10.1016/j.bmcl.2008.10.051.
[159] M. Cho, M.S. Han, C. Ban, Detection of mismatched DNAs via the binding affinity of MutS using a gold nanoparticle-based competitive colorimetric method, Chem. Commun. 125 (2008), http://dx.doi.org/10.1039/b811346g, 4573–3.
[160] W. Zhao, J.C.F. Lam, W. Chiuman, M.A. Brook, Y. Li, Enzymatic cleavage of nucleic acids on gold nanoparticles: a generic platform for facile colorimetric biosensors, Small 4 (2008) 810–816, http://dx.doi.org/10.1002/smll.200700757.
[161] W.-H. Wu, M. Li, Y. Wang, H.-X. Ouyang, L. Wang, C.-X. Li, et al., Aptasensors for rapid detection of Escherichia coli O157:H7 and Salmonella typhimurium, Nanoscale Res. Lett. 7 (2012) 658, http://dx.doi.org/10.1186/1556-276X-7-658.
[162] J.R. Carter, V. Balaraman, C.A. Kucharski, T.S. Fraser, M.J. Fraser, A novel dengue virus detection method that couples DNAzyme and gold nanoparticle approaches, Virol. J. 10 (2013) 201, http://dx.doi.org/10.1186/1743-422X-10-201.
[163] E. Mokany, S.M. Bone, P.E. Young, T.B. Doan, A.V. Todd, MNAzymes, a versatile new class of nucleic acid enzymes that can function as biosensors and molecular switches, J. Am. Chem. Soc. 132 (2010) 1051–1059, http://dx.doi.org/10.1021/ja9076777.
[164] K. Zagorovsky, W.C.W. Chan, A plasmonic DNAzyme strategy for point-of-care genetic detection of infectious pathogens, Angew. Chem. Int. Ed. 52 (2013) 3168–3171, http://dx.doi.org/10.1002/anie.201208715.
[165] S. Zhang, W. Guo, J. Wei, C. Li, X.-J. Liang, M. Yin, Terrylenediimide-based intrinsic theranostic nanomedicines with high photothermal conversion efficiency for photoacoustic imaging-guided cancer therapy, ACS Nano 11 (2017) 3797–3805, http://dx.doi.org/10.1021/acsnano.6b08720.
[166] T. Yang, Y. Tang, L. Liu, X. Lv, Q. Wang, H. Ke, et al., Size-dependent Ag 2S nanodots for second near-infrared fluorescence/photoacoustics imaging and simultaneous photothermal therapy, ACS Nano 11 (2017) 1848–1857, http://dx.doi.org/10.1021/acsnano.6b07866.
[167] B. Pelaz, C. Alexiou, R.A. Alvarez-Puebla, F. Alves, A.M. Andrews, S. Ashraf, et al., Diverse applications of nanomedicine, ACS Nano 11 (2017) 2313–2381, http://dx.doi.org/10.1021/acsnano.6b06040.
[168] V. Raeesi, L.Y.T. Chou, W.C.W. Chan, Tuning the drug loading and release of DNA-assembled gold-nanorod superstructures, Adv. Mater 28 (2016) 8511–8518, http://dx.doi.org/10.1002/adma.201600773.
[169] A.O. Govorov, H.H. Richardson, Generating heat with metal nanoparticles, Nano Today 2 (2007) 30–38, http://dx.doi.org/10.1016/S1748-0132(07)70017-8.
[170] Z. Qin, W.C.W. Chan, D.R. Boulware, T. Akkin, E.K. Butler, J.C. Bischof, Significantly improved analytical sensitivity of lateral flow immunoassays by using thermal contrast, Angew. Chem. Int. Ed. 51 (2012) 4358–4361, http://dx.doi.org/10.1002/anie.201200997.
[171] Y. Wang, Z. Qin, D.R. Boulware, B.S. Pritt, L.M. Sloan, I.J. González, et al., Thermal contrast amplification reader yielding 8-fold analytical improvement for disease detection with lateral flow assays, Anal. Chem. 88 (2016) 11774–11782, http://dx.doi.org/10.1021/acs.analchem.6b03406.
[172] W.C.W. Chan, B. Udugama, P. Kadhiresan, J. Kim, S. Mubareka, P.S. Weiss, et al., Patients, here comes more nanotechnology, ACS Nano 10 (2016) 8139–8142, http://dx.doi.org/10.1021/acsnano.6b05610.
[173] K. Ming, J. Kim, M.J. Biondi, A. Syed, K. Chen, A. Lam, et al., Integrated quantum dot barcode smartphone optical device for wireless multiplexed diagnosis of infected patients, ACS Nano 9 (2015) 3060–3074, http://dx.doi.org/10.1021/nn5072792.
[174] T. Laksanasopin, T.W. Guo, S. Nayak, A.A. Sridhara, X. Shi, O.O. Olowookere, et al., A smartphone dongle for diagnosis of infectious diseases at the point of care, Science 7 (2015) 1–10.
[175] J. Gao, X. Huang, H. Liu, F. Zan, J. Ren, Colloidal stability of gold nanoparticles modified with thiol compounds: bioconjugation and application in cancer cell imaging, Langmuir 28 (2012) 4464–4471, http://dx.doi.org/10.1021/la204289k.
[176] P.K. Drain, E.P. Hyle, F. Noubary, K.A. Freedberg, D. Wilson, W.R. Bishai, et al., Diagnostic point-of-care tests in resource-limited settings, Lancet Infect. Dis.

14 (2014) 239–249, http://dx.doi.org/10.1016/S1473-3099(13)70250-0.
[177] C. Torres, Rapid, Cheap HIV Test Finds Success as First of its Kind Tested in the Field, The Washington Post, 2011, https://www.washingtonpost.com/national/health-science/rapid-cheap-hiv-test-finds-success-as-first-of-its-kind-tested-in-the-field/2011/07/27/gIQAUo1dlI_story.html. (Accessed 2 August 2017).
[178] C.D. Chin, T. Laksanasopin, Y.K. Cheung, D. Steinmiller, V. Linder, H. Parsa, et al., Microfluidics-based diagnostics of infectious diseases in the developing world, Nat. Med. 17 (2011) 1015–1019, http://dx.doi.org/10.1038/nm.2408.
[179] D. Ioannou, D.K. Griffin, Nanotechnology and molecular cytogenetics: the future has not yet arrived, Nano Rev. 1 (2010) 5117, http://dx.doi.org/10.3402/nano.v1i0.5117.
[180] J. Li, H. Guo, Z.-Y. Li, Microscopic and macroscopic manipulation of gold nanorod and its hybrid nanostructures [Invited], Phot. Res. 1 (2013) 28–41, http://dx.doi.org/10.1364/PRJ.1.000028.
[181] K. Kerman, M. Saito, S. Yamamura, Y. Takamura, E. Tamiya, Nanomaterial-based electrochemical biosensors formedical applications, Trends Anal. Chem. 27 (2008) 585–592, http://dx.doi.org/10.1016/j.trac.2008.05.004.
[182] D. Vilela, M.C. González, A. Escarpa, Sensing colorimetric approaches based on gold and silver nanoparticles aggregation: chemical creativity behind the assay. A review, Anal. Chim. Acta 751 (2012) 24–43, http://dx.doi.org/10.1016/j.aca.2012.08.043.